ANL-6732
Reactor Technology

ARGONNE NATIONAL LABORATORY
9700 South Cass Avenue
Argonne, Illinois 60439

# CRITICAL STUDIES OF A 440-LITER FAST-REACTOR CORE FUELED WITH URANIUM ENRICHED TO 17 PERCENT (ZPR-3 ASSEMBLY 41)

by

A. L. Hess, J. M Gasidlo, J K. Long,*
P I. Amundson, and W. P. Keeney

Applied Physics Division

June 1971



*EBR-II Project

## DISCLAIMER

# TABLE OF CONTENTS

# TABLE OF CONTENTS

# TABLE OF CONTENTS

# LIST OF FIGURES

# LIST OF FIGURES

# LIST OF FIGURES

# LIST OF TABLES

# LIST OF TABLES

# LIST OF TABLES

# CRITICAL STUDIES OF A 440-LITER FAST-REACTOR CORE FUELED WITH URANIUM ENRICHED TO 17 PERCENT (ZPR-3 ASSEMBLY 41)

by

A. L. Hess, J. M. Gasidlo, J. K. Long,
P. I. Amundson, and W. P. Keeney

## ABSTRACT

ZPR-3 Assembly 41 was a cylindrical fast-reactor system composed of a dilute uranium core surrounded by a thick, depleted-uranium blanket. The fuel, a five-to-one mixture of $^{238}U$ and $^{235}U$, amounted to 35 vol % of the core, and this was diluted with 18 vol % aluminum, 14 vol % steel, and 33 vol % void. A critical mass of 494 kg of $^{235}U$ was measured for this composition. Basic physics experiments included measurements of spectral indices, material reactivity coefficients, and flux profiles. The worths of steel and aluminum as reflectors, relative to uranium, were investigated in radial and axial blanket regions. Studies were carried out to determine the relative merits of three breeder-blanket concepts: an EBR-II-type blanket (with 40 vol % uranium, 40 vol % sodium, and 20 vol % steel); a UC type blanket (with 20 vol % uranium, 20 vol % carbon, 40 vol % sodium, and 20 vol % steel), and a two-zone blanket with an inner zone of EBR-II-type blanket and an outer zone containing graphite instead of uranium. Worths of boron carbide near the core in two blanket types were measured to evaluate a rotary-control-rod concept for fast reactors. This report contains experimental details and the results of all measurements.

## I. INTRODUCTION

Assembly 41 in Argonne's Zero Power Reactor 3 was a dilute, uranium-fueled fast-reactor system. The core was composed of 35 vol % uranium, with a $^{238}U/^{235}U$ ratio of about five, diluted with aluminum and steel. This composition was studied to augment a series of other ZPR-3 assemblies in which a similar volume fraction of uranium was used, but with $^{238}U/^{235}U$ ratios ranging between one and 10. This assembly was also of interest for the comparison of experimental results with measurements made in a fast exponential experiment and in a fast thermal critical assembly, both of which used a similar 5/1 composition.

In addition to the determination of critical mass, the experiments with Assembly 41 included measurements of basic reactor-physics properties, spectral indices, comparative worths of different reflector materials, and the relative merits of some EBR-II blanket concepts. This report presents the essential details and results of the experiments in formats intended to facilitate inputs to reactor-calculation codes. Comparisons are made, where valid, between the results in Assembly 41 with those of similar experiments in the 5/1 exponential and fast-thermal systems. Some correlations of experimental results with values provided by diffusion-theory calculations are also included.

The Assembly 41 program was carried out between August 20, 1962, and October 15, 1962, by personnel of the ZPR-3 facility of Argonne's Idaho Division.

# II. ASSEMBLY 41 CRITICAL EXPERIMENT

## A. The ZPR-3 Facility

Zero Power Reactor 3 (ZPR-3), shown in Fig. 1, is a split-halves critical-assembly machine for the study of fast-reactor systems. The machine halves, one fixed and one movable, each consist of an array of matrix tubes into which drawers are inserted. A variety of materials in plate or block form are available for loading into the drawers to achieve the desired representation of a fast-reactor core and blanket.

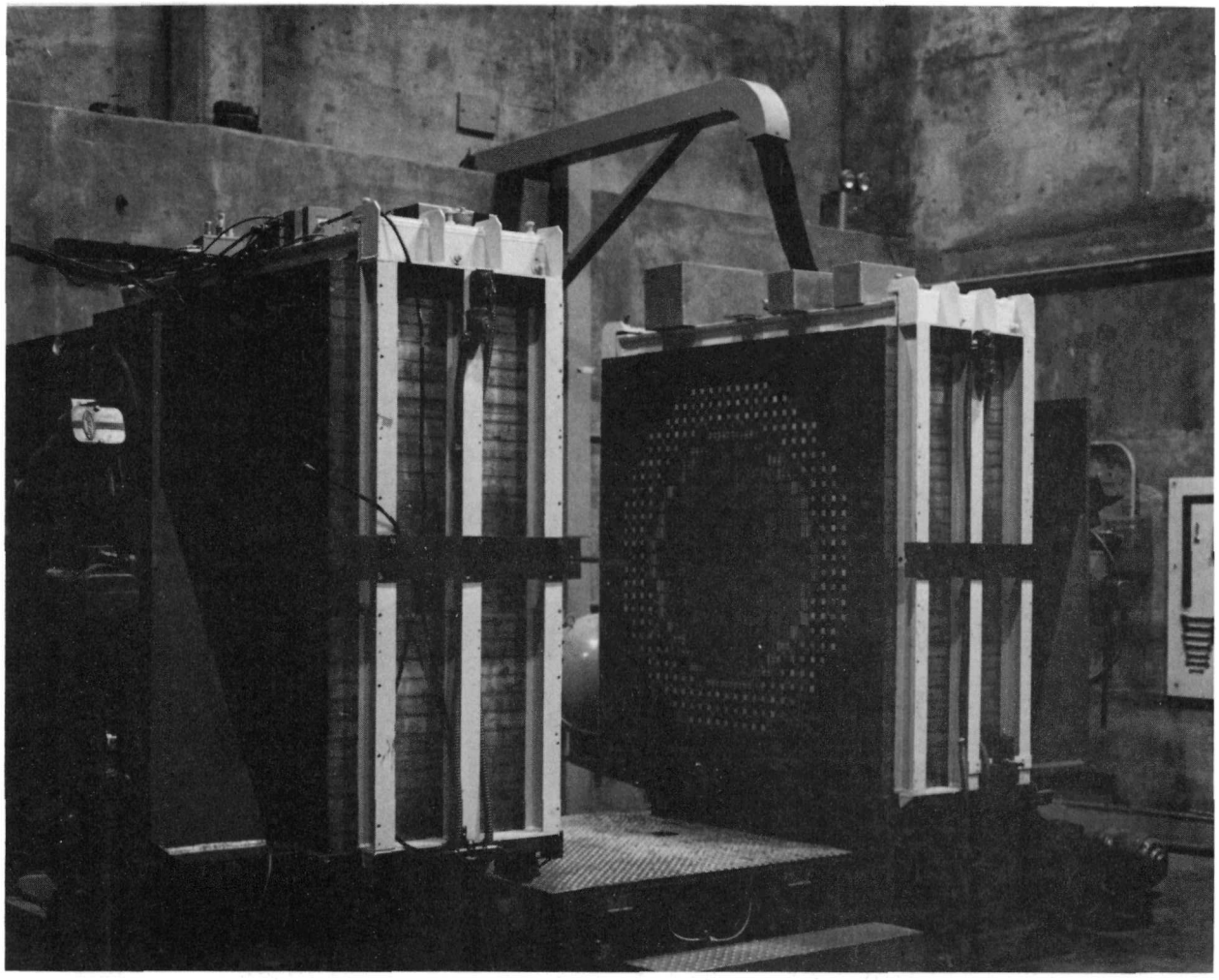

Fig. 1. View of ZPR-3 Critical Facility. ANL Neg. No. 103-2215.

Figure 2 illustrates typical loadings of drawers. The construction, instrumentation, and operation of the facility have been described by Cerutti et al.[1] and by Long.[2] Besides studies of simple, fast-reactor systems, ZPR-3 has been used for mockups of several fast-power-reactor designs.

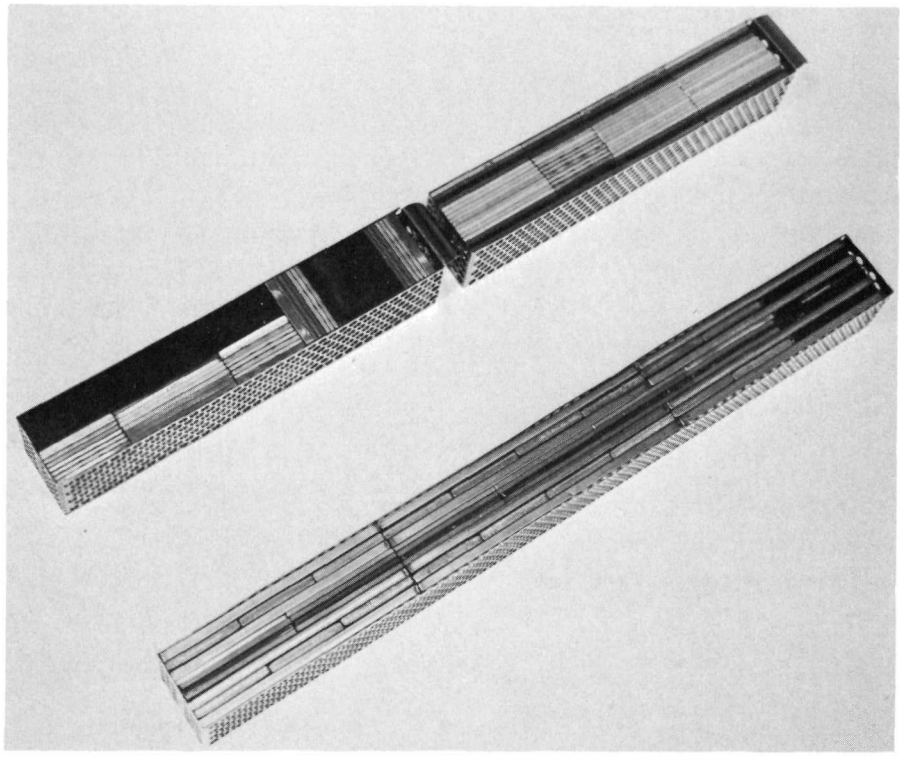

Fig. 2. Typical Core and Axial Blanket Drawers. ANL Neg. No. 103-2231.

## B. Design of Core and Blanket Regions of Assembly 41

The prime objective in designing the Assembly 41 core was to obtain a $^{235}U$ volume fraction as close as practical to the fraction in the exponential experiments; this was achieved by using a four-drawer sequence containing five 1/8-in.-thick columns of enriched uranium as the basic cell for the Assembly 41 core. Depleted uranium, steel, and low-density aluminum plates were added as diluents to complete the composition. Figure 3 shows the arrangement of the materials across the four drawers in the sequence; this sequence was loaded into the reactor matrix in a repetitive fashion horizontally across the core to effectively achieve vertical planes of fuel columns evenly separated by about four-fifths of a drawer width. Preliminary calculations suggested a core size of 480 liters, and on this basis the core length was set at 32 in. to obtain a length-to-diameter ratio of 0.9. Thus the loading of core materials in the drawers shown in Fig. 3 extended for 16 in. axially, and this was followed by 5 in. of depleted-uranium axial blanket in the 21-in.-length front drawer and another 7 in. of blanket in backup drawers. A radial blanket was also constructed from depleted uranium (in the form of 2 x 2 x 2- or 2 x 2 x 5-in. bricks). The ZPR-3 control rods consisted of special movable drawers in the core; these drawers contained materials as in the four-drawer sequence, except for a slightly different amount of steel.

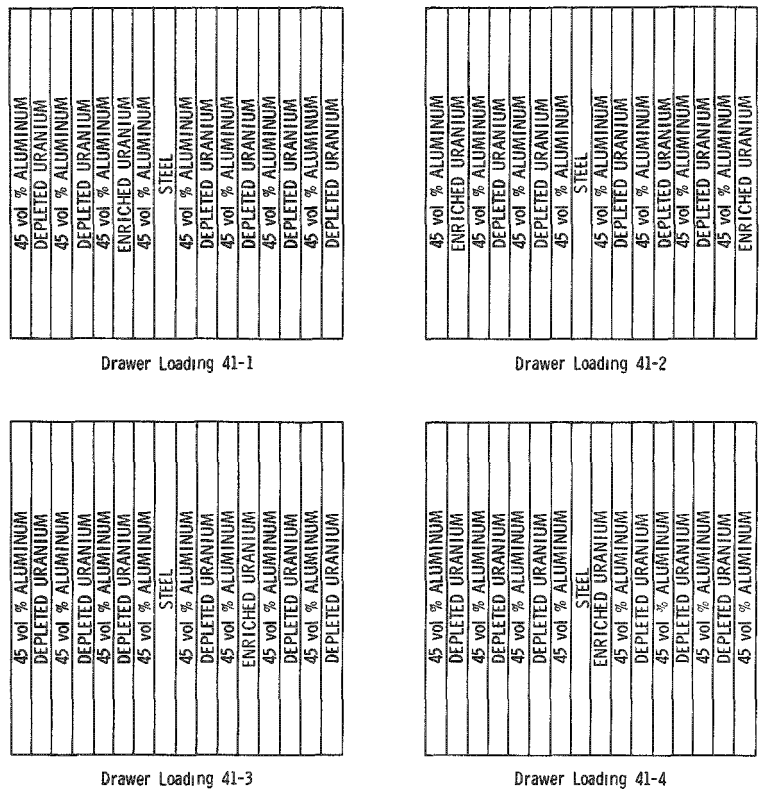


Fig. 3. Four-drawer Sequence Used for Assembly 41 Core

Appendix A gives material-loading specifications for all drawers involved in the basic design of Assembly 41. Atom densities and thicknesses for the material columns in the four-drawer cell sequence used in the core are given in Appendix B to specify the heterogeneous aspect of the core. The average four-drawer cell composition is given in Table I in

TABLE I Regional Specifications for ZPR 3 Assembly 41

| Region / Specification | Four-drawer-cell Composition | As-built Reference Core | Axial Blankets[a] | Axial Spring Gaps[a] | Inner Radial Blanket (in drawers) | Outer Radial Blanket (in matrix) |
|---|---|---|---|---|---|---|
| Average Composition $10^{22}$ atoms/cm$^3$ | | | | | | |
| $^{235}U$ | 0 2817 | 0 2864 | 0 0083 | - | 0 0083 | 0 0084 |
| $^{238}U$ | 1 4008 | 1 3964 | 3 9892 | | 3 9897 | 3 9956 |
| $^{236}U$ | 0 0012 | 0 0012 | - | - | | - |
| $^{234}U$ | 0 0029 | 0 0029 | | - | | - |
| Aluminum | 1 0784 | 1 0785 | - | | | |
| Iron | 0 8748 | 0 8774 | 0 5703 | 1 685 | 0 5639 | 0 4540 |
| Chromium | 0 2176 | 0 2183 | 0 1419 | 0 419 | 0 1403 | 0 1129 |
| Nickel | 0 0952 | 0 0955 | 0 0621 | 0 184 | 0 0614 | 0 0494 |
| Manganese | 0 0091 | 0 0091 | 0 0059 | 0 018 | 0 0059 | 0 0047 |
| Silicon | 0 0108 | 0 0107 | 0 0070 | 0 020 | 0 0069 | 0 0055 |
| Average Dimensions | | | | | | |
| Length cm | 81 43 | 81 43 | 12 70 17 78[a] | 0 66 | 106 83[b] | 142 24[b] |
| Radius cm | 41 90[c] | 41 55 | 41 55 | 41 55 | 51 94 | 75 02 |
| Volume liters | 449 1[c] | 441 7 | 68 9 96 4[a] | 5 6 | 326 | 983 |
| Unadjusted Criticality Specifications[d] | | | | | | |
| $^{235}U$ loading kg | 493 75 | 493 75 | | | | |
| Excess reactivity ¢h | 47 ± 2 | 61 4 ± 0 7 | | | | |

[a]Spring gaps at ends of the 21-in front drawers divide each of the axial blankets into two sections a 5 in (12 70-cm) length beyond the core in the front drawer and a 7-in (17 78-cm) length in the backup drawers See Fig 8 (later) for pictorial representation
[b]See Fig 8 (later) for geometric details
[c]Adjusted to give cell-composition $^{235}U$ concentration for as-built $^{235}U$ loading
[d]As-built No corrections applied for core-edge irregularity interface irregularity or core material heterogeneity

atoms/cm$^3$ and is equivalent to about 5.86 vol % $^{235}$U, 29.2 vol % $^{238}$U, 14.1 vol % steel (Type 304 stainless), 17.9 vol % aluminum, and 32.9 vol % void. The radial and axial blankets, also specified in Table I, contained about 83 vol % uranium and 9 vol % steel.

## C. Approach to Critical and Reference Configuration

In the initial loading, fueled core drawers were loaded radially out from the axis to about 40% of the expected 480 liter critical volume. The remaining drawers of the expected volume were loaded as "dummy" core drawers in which columns of 63 vol % aluminum plates (perforated) were installed in place of the enriched-uranium plates. A radial blanket of depleted uranium with an average thickness of about 12 in. was placed around the expected core configuration.

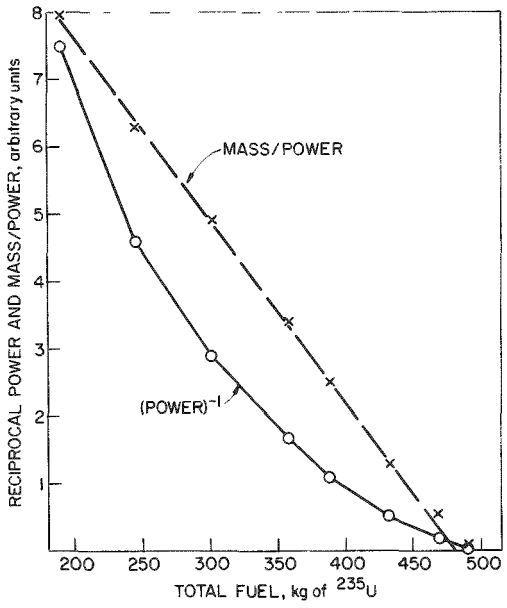


Fig. 4. Approach-to-critical Curves

The approach to critical was made by stepwise increases of the radius of the active core, replacing the 63 vol % aluminum columns in the dummy drawers with enriched uranium. Criticality was achieved in the ninth loading with a total of 496 kg of $^{235}$U in 444 liters. The approach-to-critical history is plotted in Fig. 4 as the reciprocal of the power (as obtained from $^{10}BF_3$ proportional counters located in the blanket in drawers 1-I-12 and 2-T-9) versus the core $^{235}$U loading.

About 30 dummy core drawers remained around the active core in the initial critical loading, and these were replaced with depleted-uranium radial blanket drawers. Other irregularities were removed, and a clean-core critical loading was established. This "reference" configuration is shown in the ZPR-3 interface views in Figs. 5 and 6. Details of the loading are included in Appendix A. The total fuel in the reference loading was 493.8 kg of $^{235}$U, and the available excess reactivity was determined from later rod calibrations to be 61.4 ± 0.5 Ih. The as-built critical system was therefore a cylindrical core with a heterogeneous structure as indicated in Fig. 3 and a stepped boundary as shown in Figs. 5 and 6, and the experimental multiplication constant (k) (with all rods inserted) was 1.0014 ± 0.0001.

This reference configuration contained uneven amounts of the four types of drawer loadings comprising the basic core cell shown in Fig. 3. The type present in greatest amount was the Type-2 drawers (with two enriched-uranium columns); therefore the average composition had a higher

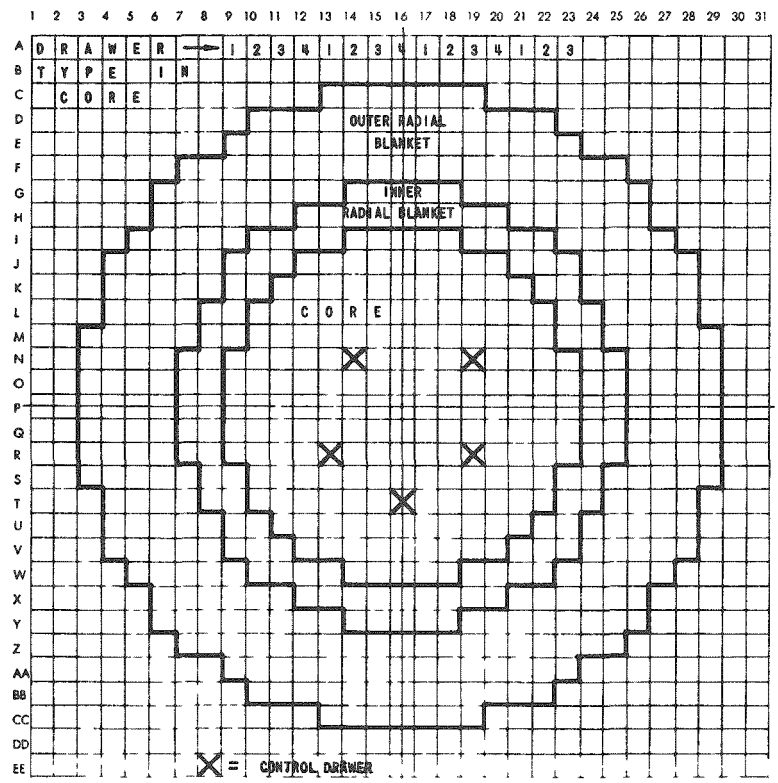


Fig. 5. Interface View of Half 1 of Assembly 41, Reference Critical Configuration

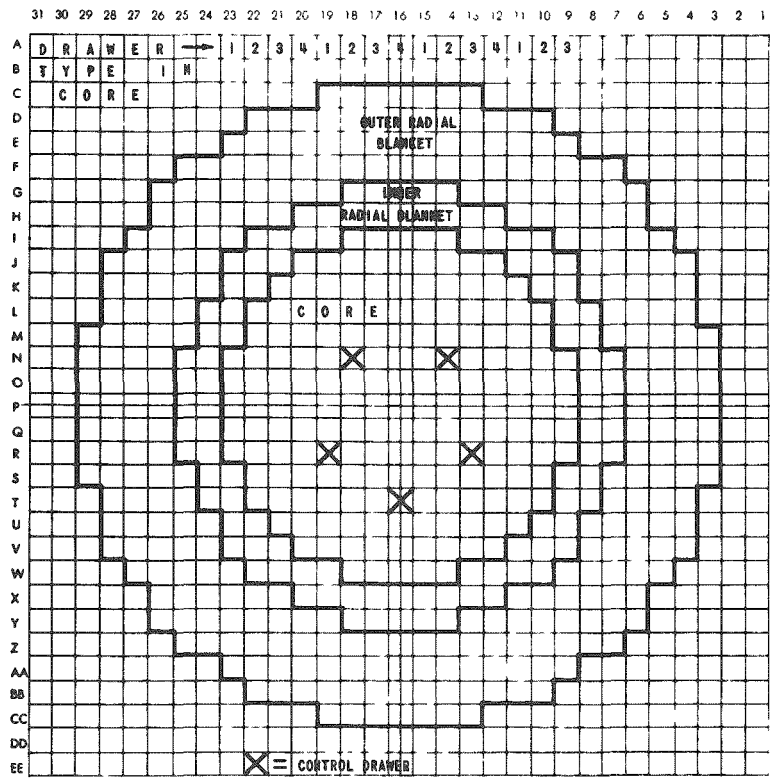


Fig. 6. Interface View of Half 2 of Assembly 41, Reference Critical Configuration

density of $^{235}U$ than the four-drawer cell. Table I includes this average as-built composition. However, the effective $^{235}U$ concentration is determined by the average spacing between enriched-uranium columns, which in the as-built core is the same as in the four-drawer cell. For calculations of the reactor characteristics, it is therefore appropriate to use core models based on the four-drawer cell composition. Corrections to the as-built core to provide the desired models are developed in Section E below.

## D. Reactivity of Fuel at Edge of Core

Determining the average worth of core material replacing blanket material at the boundary was complicated by the nature of the basic core cell (containing five enriched-uranium columns in four drawers). The worth of core medium (without enriched uranium) replacing depleted-uranium blanket was derived from the earlier replacement of dummy core drawers by radial blanket in the construction of the clean critical configuration (see Section II.C); an average value of -2.15 Ih per drawer of diluent was obtained in the replacement. Then, throughout the program of worth measurements in the assembly, there were several exchanges of core drawers of all four types with blanket drawers at locations around the core periphery. Assuming a constant worth for the diluent materials replacing blanket (-2.15 Ih/drawer), average worths of the enriched-uranium columns contained were then deduced from the measured worths of the full core drawers. Figure 7 shows the results of these fuel-worth measurements as a function of radius near the core-blanket boundary.

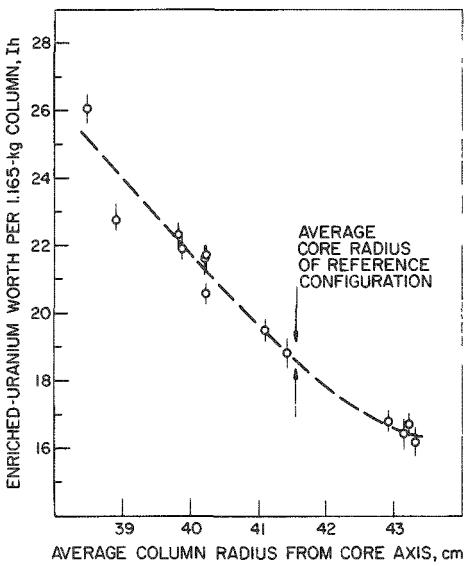


Fig. 7. Fuel-column Worth vs Radius near Radial Edge of Core

Next to be considered was the variation of enriched-uranium worth near the core edge. The core edge was taken to be at a radius of 41.55 cm, the radius of a smooth cylinder of the same cross-sectional area as the core; at this point of the curve in Fig. 7, the worth of an enriched-uranium column could be defined by the linear relationship

$$\text{Worth (per column)} = (95.52 - 1.85r)\ \text{Ih},$$

where

$r$ = radius in centimeters.

For a cell containing five columns of enriched uranium, the edge worth of core material (including the worth of four drawers of diluent) was then expressed by the relationship

$$\text{Core-material worth} = (85.47 - 1.6886r)\ \text{Ih/kg of contained } ^{235}\text{U}$$

(for $^{235}$U plus associated diluent replacing uranium radial blanket). At the area-equivalent radius of 41.6 cm, the relationship gives the core-edge fuel worth of 15.33 ± 0.80 Ih per kg of $^{235}$U. Using a conversion factor of 440 Ih per % $\Delta k/k$, the fuel-mass equivalence to reactivity becomes

$$\Delta M/M = 5.8\ \Delta k/k$$

E Evaluation of the Critical Size for a Heterogeneous Cylindrical Core with the Four-drawer Cell Composition

A number of adjustments are required to the as-built critical configuration of the core to derive an experimentally based model for reactor calculations with the average basic-cell composition. First, diluent must be added around the core periphery to obtain a total volume fraction of diluent equal to that of the basic cell Next, core material must be removed to compensate for the excess reactivity of the loading and the worths of various necessary transitions from the as-built situation to a smooth circular-cylinder model. The total reactivity correction arises from four adjustments.

1 The available excess reactivity of the reference configuration, plus the worth of the added edge diluent

2 The worth of the interface gap.

3 The worth of the core-edge irregularity.

4 The worth of the extra steel in the control drawers.

In detail, these adjustments are evaluated as follows.

1 Excess Reactivity

For the reference loading of 493.8 kg of $^{235}$U, the excess reactivity was 61 4 ± 0.6 Ih and the volume was 441.7 liters. Based on the $^{235}$U density in the four-drawer cell, the core volume should have been 449.2 li ters The addition of 7.5 liters of diluent, replacing uranium blanket, around the core periphery would have decreased the reactivity by 12.9 Ih For a 493.8-kg, 449.1-liter core with the four-drawer cell composition, the available excess reactivity would thus have been 48.5 ± 0.8 Ih.

2. Worth of Interface Gap

The fronts of the loading drawers constitute a 0.152-cm gap of steel and void which separates the core materials in the two halves of the reactor. In computing the average cell composition and establishing an

axially-uniform core model, we have homogenized the gap over the full length of the core, and the average fuel concentration has been slightly diminished to fill the gap. Therefore, the model has a reactivity advantage over the real situation. This reactivity advantage is equal to the amount by which the worth of the fuel in the gap exceeds the worth of the same fuel distributed uniformly throughout the core. The average worth of $^{235}U$ at the core midplane was estimated as 76 ± 6 Ih/kg, and the average worth throughout the core was estimated as 47 ± 5 Ih/kg. With a net effect of fuel translation of 29 ± 7 Ih/kg and a gap content of 0.93 kg of $^{235}U$, the homogenization in the model is worth 27 ± 7 Ih.

3 Worth of Edge Irregularity

A smooth cylindrical model, with radius determined on the basis of cross-sectional area for the as-built stepped-outline cylinder, has a reactivity advantage due to the net transfer of fuel from outside the radial boundary to inside. This transfer worth is computed by an approximate formulation

$$W_t = \Delta M \cdot \bar{d} \cdot \left(\frac{dW}{dr}\right)_{r_e},$$

where

$\Delta M$ = mass of fuel protruding beyond equivalent area circle,

$\bar{d}$ = the average displacement of fuel in the transfer from outside to inside the circle,

and

$\left(\frac{dW}{dr}\right)_{r_e}$ = the derivative of the fuel worth as a function of radius at the equivalent-area radius $r_e$.

In terms of the cross-sectional area, A, of the core, and the protruding area, $\Delta A$,

$$\Delta M = M\Delta A/A,$$

where

$M = 494$ kg $^{235}U$.

By geometric analysis of the core outline, $\Delta A/A = 0.025$, the average radial protrusion of drawer corners beyond $r_e$ is 2.07 cm, and the average intrusion of corners inside of $r_e$ is 2.10 cm. Considering the protruding and

intruding drawer segments as triangles, the average displacement of fuel from outside to inside the equivalent area circle would be

$$\bar{d} = \tfrac{1}{3}(2.07 + 2.10) = 1.39 \text{ cm.}$$

Using $dW/dr = 1.69 \pm 0.35$ Ih/kg-cm gives a worth of $+29.0 \pm 6.0$ Ih for smoothing the radial core boundary.

4. Worth of Extra Steel in Control Drawers

An excess steel content of 1.39 kg in the control drawers must be removed to obtain the steel composition of the four-drawer cell. Using a steel worth of $+1.5 \pm 1$ Ih/kg in the average rod positions (estimated on the basis of steel worths measured at the core center and core edge) gives a correction of $-2.1 \pm 1.4$ Ih.

After the four above adjustments are made, the excess reactivity for the heterogeneous model with the dilution-corrected volume of 449 liters totals $102.4 \pm 9.4$ Ih. The removal of an equivalent worth of fuel would take place in the radial region between 41.9 and 41.6 cm, where the average worth of core material is $14.0 \pm 0.9$ Ih/kg of $^{235}U$; this gives a just-critical $^{235}U$ mass of $486.5 \pm 0.9$ kg for a smooth heterogeneous cylinder with the composition of the basic four-drawer cell. The just-critical volume, 442.53 liters, would mean a radius of 41.59 cm with the core length of 81.43 cm. As a k = 1 model, the estimated uncertainty is $\pm 0.0004$ $\Delta k/k$, based on probable experimental errors. Figure 8 shows the geometry for this model.

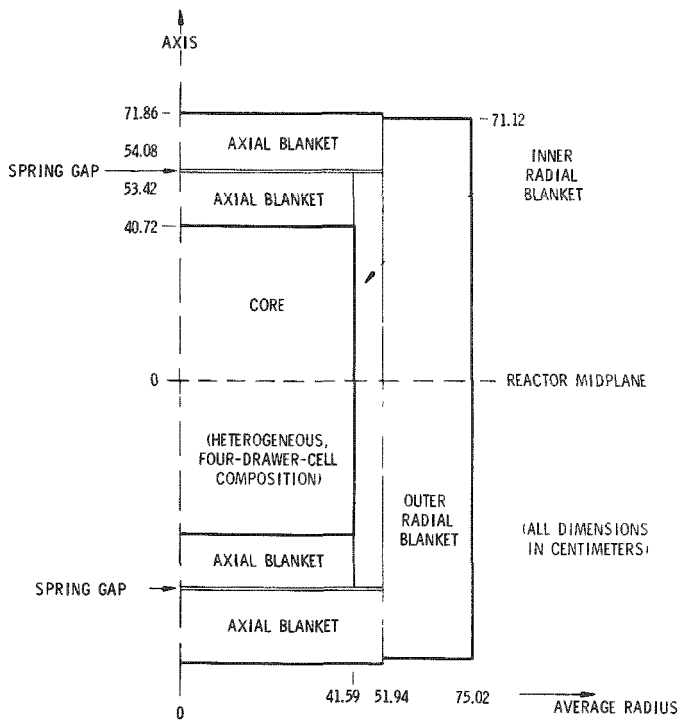


Fig. 8. Axial Schematic Diagram for Cylindrical Representation of Assembly 41

## F. Evaluation of the Critical Size for a Homogeneous Cylinder with the Average Composition of the Four-drawer Cell

The results of heterogeneity studies, reported in Section III, indicated that the presence of the enriched uranium in the form of 1/8-in.-thick plates provided a reactivity advantage of 323 ± 30 Ih over having a uniform dispersal of the fuel. The conversion to a homogeneous model therefore requires an increase in the core volume to compensate for the reactivity lost in "homogenization" of the fuel. An adjustment for the decreased reactivity of homogeneous fuel to the previously cited edge-fuel-worth relationship gives the equation

$$\text{homogeneous-fuel worth} = (84.28 - 1.66r)\ \text{Ih/kg of } ^{235}\text{U}.$$

Over the range in radius of the compensating increase in volume, the average core material worth becomes 14.34 ± 1.5 Ih/kg of $^{235}$U and the compensation amounts to 22.5 kg of $^{235}$U. Therefore, a homogeneous cylindrical core with a composition equal to the average four-drawer cell composition would have a critical mass of 509.0 ± 2 kg of $^{235}$U and a volume of 463 liters; this requires a critical radius of 42.54 cm for a length of 81.43 cm. Reactivity uncertainty for this model (k = unity) is estimated as ±0.001 Δk/k.

## G. Evaluation of the Critical Size for a Homogeneous Sphere with the Average Composition of the Four-drawer Cell

On the basis of investigations reported by Davey,[3] the "shape factor" for conversion of the cylindrical critical volume for the Assembly 41 core to an equivalent spherical volume is 0.92. When this factor is applied to the volume obtained above, a value of 426 liters is obtained for the spherical critical volume of a homogeneous core with the average composition of the four-drawer cell. The corresponding critical mass is 468 kg of $^{235}$U. The value of 462 kg given by Davey[3] was based on the as-built core composition and on different estimates of the various corrections.

The equivalent sphere has a radius of 46.68 cm, and the uncertainty in the applied shape factor is probably ±0.015. The uncertainty in reactivity is therefore estimated as ±0.003 Δk/k for this k = 1, one-dimensional model.

## H. Control-rod Calibrations

A ZPR-3 control drawer loaded as a normal core drawer, in matrix location 1-N-14 (Fig. 5), was used as the principal reactivity-balancing device for worth measurements in Assembly 41. It was calibrated by making period measurements to obtain the reactivity content of successive rod displacements. A graph of this calibration (Fig. 44) is included in Appendix C.

Appendix C also presents the delayed-neutron characteristics for this assembly as obtained from diffusion-theory calculations. The principal values obtained were an effective delayed-neutron fraction of 0.0073, and a conversion factor of 440 Ih per % Δk/k.

# III. FUEL-HETEROGENEITY EXPERIMENTS

Fuel "bunching" and "unbunching" experiments were undertaken in the core to evaluate the reactivity advantage of fuel in the form of 1/8-in.-thick plates over the reactivity of a homogeneous core with the same average composition.

## A. Fuel Bunching

For the bunching experiment, the normal arrangement of the enriched-uranium columns, spaced every four-fifths of a drawer in the cell sequence, was altered to produce 1/4-in. columns spaced every $1\frac{3}{5}$ drawers. The transition involved is illustrated in Fig. 9. Only part of the total core fuel was bunched, that which was contained in the two radial sectors of half No. 1 shown in Fig. 10. A total of 38 regular columns were bunched into nineteen 1/4-in.-thick columns (double 1/8-in. columns). With 44.25 kg of enriched uranium transposed, the bunching effect was a reactivity gain of 52.25 ± 1.0 Ih.

## B. Fuel Unbunching

The reference loading for the unbunching experiment contained the normal fuel-column arrangement throughout the core, however with a number of the 1/8-in. columns consisting of two columns of 1/16-in.-thick plates. In the unbunching, the double 1/16-in. enriched-uranium columns spaced four-fifths of a drawer apart were separated into 1/16-in. columns spaced two-fifths of a drawer apart. Figure 11 shows the radial sector of the core involved in this experiment. The unbunching of 23 double columns into

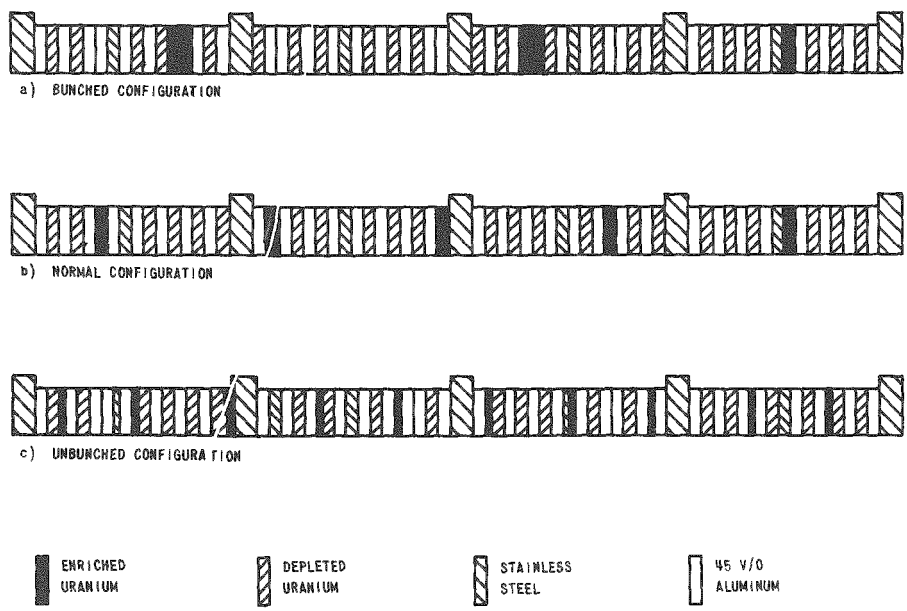


Fig. 9. Four-drawer-cell Plate Arrangements for Heterogeneity Experiments

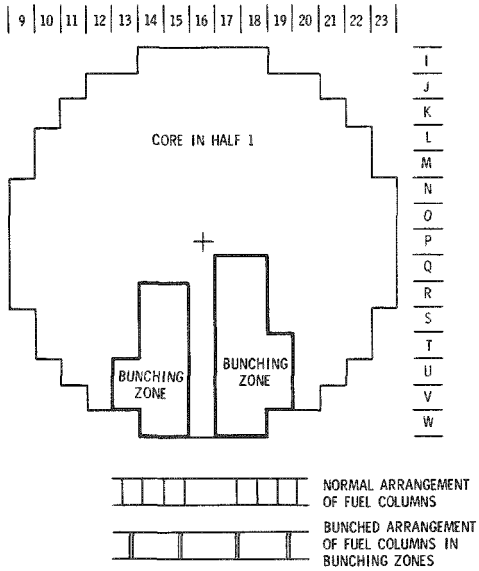


Fig. 10. Outline of Core Zones Used in Fuel-bunching Experiment

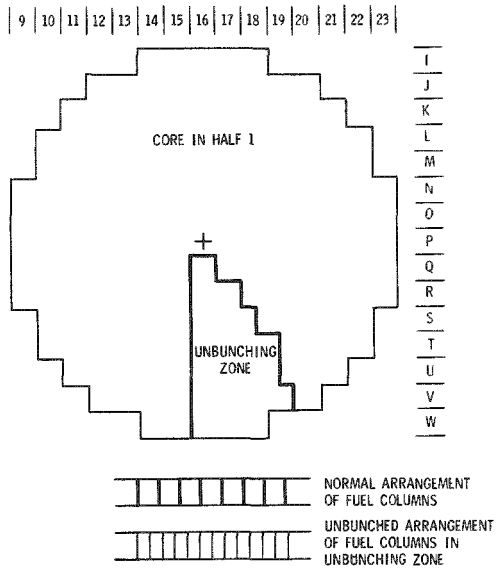


Fig. 11. Outline of Core Zone Used in Fuel-unbunching Experiment

46 separate 1/16-in. columns was worth -8.4 ± 0.8 Ih; the fuel mass so moved was 26.82 kg of enriched uranium.

## C. Extrapolation to Homogeneous Core

The zones involved in the heterogeneity experiments approximated radial sectors of the core and thus had average material-worth characteristics about the same as in the entire core. On this basis, a linear extrapolation of the results of the heterogeneity experiments to the full content of enriched uranium in the core should therefore be reasonable. For the "clean" just-critical configuration (see Section II.E), there would be 516.2 kg of enriched uranium as 1/8-in.-thick columns. The extrapolated bunching effect, with all the fuel in 1/4-in.-thick columns, would then be +610 ± 12 Ih, or +1.40 ± 0.02% Δk/k. In unbunching all of the core fuel into 1/16-in. plates, there would be a reactivity loss of 161.7 ± 15 Ih. These results are plotted in Fig. 12 as relative worth versus fuel-column thickness. The heterogeneity advantage factor sought is the reactivity difference between the 1/8-in. normal Assembly 41 fuel configuration and the zero-thickness or homogeneous situation. An extrapolation on the graph gives a value of 323 ± 30 Ih for this factor, or 0.734 ± 0.035% Δk/k.

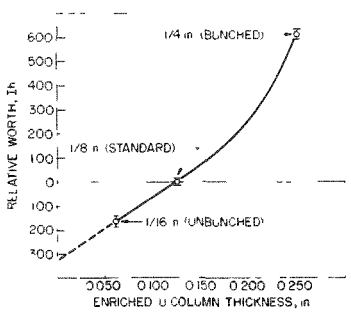


Fig. 12

Heterogeneity Worth vs Fuel-plate Thickness for Full-core Extrapolation

# IV. ROSSI ALPHA

Rossi alpha, the ratio of the effective delayed-neutron fraction to the prompt-neutron lifetime, was measured in Assembly 41 using the technique described by Brunson.[4] Decay constants for prompt-neutron die-away were measured at several subcritical states, and an extrapolation was made to obtain a value of $\alpha = -5.55 \times 10^{4}$ sec$^{-1}$ at delayed critical. For these experiments, subcritical states approaching -400 Ih were achieved by withdrawal of control rods and removal of fuel from the core. The low multiplications then required operation with the startup sources in the reactor to give adequate counting rates.

The calculated effective delayed-neutron fraction ($\beta_{eff}$) was 0.0073, and the measured alpha value thus indicates a prompt-neutron lifetime of $13.2 \times 10^{-8}$ sec.

# V. REACTIVITY-COEFFICIENT MEASUREMENTS

The worths of materials at the core center and at the radial edge of the core near the midplane were measured by a series of replacement experiments. The materials included fuels and structural elements of relevance to fast reactors and also numerous other materials with high neutron-capture or -scattering properties. The influence of sample size on the measured reactivity coefficients was also investigated.

In all these experiments, reference runs of the reactor were made with voided sample spaces in the locations studied. The reactivity changes due to sample insertion into the void were then obtained from the differences in the critical positions determined on the calibrated control rods. The procedure thus involved a shutdown after the reference (to load the sample) and a new startup; the major source of error in most measurements was the uncertainty due to reclosure of the halves, an estimated ±0.25 Ih. Other factors contributing error were uncertainties in corrections applied for temperature drift and sample canning, and an overall rod-calibration uncertainty of ±1%.

## A. Central Worth Measurements with Small Fuel Samples

Spaces for sample substitutions at the center of the core were made by recessing the core materials away from the front of drawers 1-P-16 and 2-P-16. For fuel materials, the dimensions of the sample space were 1/4 x 2 x 2 in. in each drawer. Plates of fast-reactor fuel materials 1/4 in. thick, or 1/8 in. thick sandwiched in aluminum spacers, were inserted in place of 45 vol % aluminum in the spaces to obtain fuel worths relative to void. Figure 13 shows the configuration of a sample space.

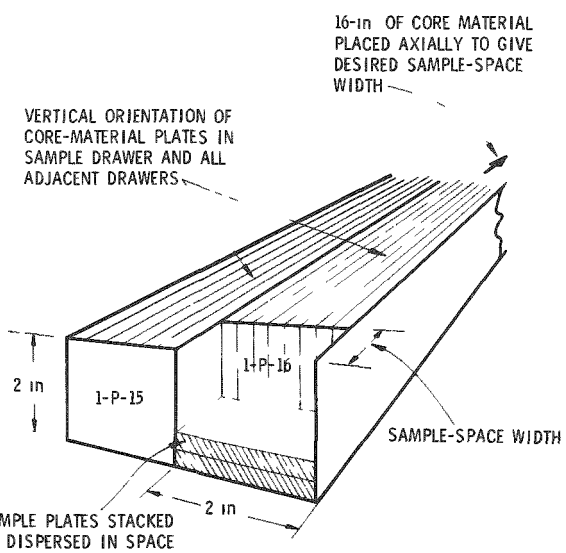


Fig. 13. Sample-space Configuration for Reactivity-coefficient Measurements

Table II gives the specifications for each material and the results of the worth measurements. The worths have been corrected for any cladding or spacer contributions. Reactivity coefficients are given as inhours per kilogram of the materials in the plate sizes used; no adjustments have been made to correct the results for self-multiplication of other sample-size effects in the plates. The table also includes breakdowns of the coefficients according to isotopic constituents, assuming linear combinations of worths.

TABLE II. Reactivity Coefficients Measured in Central 1/2 x 2 x 2-in. Sample Space

| Sample Material | Sample Mass,[a] g | Sample Worth,[a] Ih | Material Reactivity Coefficients, Ih/kg | Derived Isotopic Coefficients | |
|---|---|---|---|---|---|
| | | | | Isotope | Ih/kg |
| Enriched uranium[b] | 288 | 32.8 ± 0.3 | 114 ± 1 | $^{235}U$ | 123 ± 1 |
| Depleted uranium[c] | 595 | -3.2 ± 0.3 | -5.3 ± 0.5 | $^{238}U$ | -5.6 ± 0.5 |
| $^{233}U$ mixture[d] | 240 | 49.9 ± 0.5 | 220 ± 2 | $^{233}U$ | 225 ± 2 |
| Plutonium[e] | 186 | 37.5 ± 0.4 | 202 ± 2 | $^{239}Pu$ | 210 ± 5[f] |
| Thorium | 373 | -4.5 ± 0.3 | -12.0 ± 1.0 | $^{232}Th$ | -12 ± 1 |

[a]Excluding mass and worth of spacers or claddings.
[b]93.2 wt % $^{235}U$, 6.8 wt % $^{238}U$.
[c]0.206 wt % $^{235}U$.
[d]2.4 wt % $^{238}U$, 97.6 wt % $^{233}U$.
[e]94.5 at. % $^{239}Pu$, 5.1 at. % $^{240}Pu$, 0.4 at. % $^{241}Pu$.
[f]Assuming $^{240}Pu$ worth/kg = 20% of $^{239}Pu$ worth/kg, and $^{241}Pu$ worth/kg = $^{239}Pu$ worth/kg.

## B. Central Worth Measurements with 2-in.-cube Diluent Samples

For the less reactive materials, a 1 x 2 x 2-in. sample space was made at the front of each drawer 1-P-16 and 2-P-16. Table III gives the results of substitutions of materials into the combined 2 x 2 x 2-in. central space. For each measurement, unless otherwise noted, the cubical space was entirely filled by the samples (solid or canned). Other measurements with samples of varying size in a 2 x 2 x 2-in. space are described in Section C below. The worths and coefficients in Table III are for the materials relative to void.

## C. Effects of Sample Size on Reactivity Coefficients

Simple perturbation theory is often used to calculate the worths of infinitely dilute materials in homogeneous reactor media for comparison with measured worths. The experimental-theoretical correlations are subject to some uncertainties because of (1) the heterogeneous environment in the measurements and (2) the size and orientation of the samples. Relatively thick samples were used for the Assembly 41 experiments, and these were mostly oriented perpendicular to the columns of standard core materials in one drawer of the four-drawer sequence. As an aid to evaluating the uncertainties due to the experimental techniques, the effects of sample size were investigated with some highly reactive materials: enriched $B_4C$, enriched boron, tantalum, and polyethylene. Limited size-effect studies were also performed with depleted uranium and thorium.

### 1. Enriched-$B_4C$ Experiments

Block samples of varying thickness were constructed from 1/4 x 2 x 2-in. plates of enriched boron carbide. The worths of these samples relative to void were measured in two series of experiments: In one, the blocks of various sizes were placed at the bottom of a constant 2 x 2 x 2-in. sample space at the center; in the other, the sample space was

reconstructed to just accommodate each block size. Up to four plates were used per block. The results of both substitution series are given in Table IV, and the specific worths for the different sample thicknesses are plotted in Fig. 14.

TABLE III. Reactivity Coefficients Measured in 2-in.-cube Central Sample Space

| Sample Material | Sample Mass,[a] g | Sample Worth,[a] Ih | Material Reactivity Coefficients, Ih/kg |
|---|---|---|---|
| Ag[b] | 683 | -27.05 | -39.6 ± 0.4 |
| Al | 351 | -1.53 | -4.4 ± 0.7 |
| $Al_2O_3$ | 355 | -1.46 | -4.1 ± 0.7 |
| As | 382 | -9.83 | -25.7 ± 0.7 |
| Ba | 322 | -0.30 | -0.9 ± 0.8 |
| Be | 241 | +4.89 | +20.3 ± 1.0 |
| Bi | 1276 | -1.73 | -1.35 ± 0.20 |
| C | 196 | +0.25 | +1.28 ± 1.28 |
| $CH_2$ | 119 | +99.7 | +840 ± 0.84 |
| Cr | 439 | -1.75 | -3.98 ± 0.57 |
| Fe | 1028 | -4.51 | -4.39 ± 0.24 |
| Hf | 1653 | -30.70 | -18.6 ± 0.2 |
| Hg | 1383 | -7.52 | -5.44 ± 0.18 |
| Mo | 1280 | -12.84 | -10.0 ± 0.20 |
| Na | 91 | +0.03 | 0.3 ± 2.7 |
| Nb | 490 | -7.50 | -15.3 ± 0.5 |
| Ni | 1150 | -7.38 | -6.4 ± 0.2 |
| O | (471) | (-1.80) | -3.8 ± 0.5 |
| Physicum I[c] | 232 | -3.50 | -15.1 ± 1.1 |
| Physicum II[c] | 210 | -3.50 | -16.7 ± 1.2 |
| Ru | 228 | -4.44 | -19.5 ± 1.1 |
| S | 200 | -2.60 | -13.0 ± 1.2 |
| S[d] | 63 | -1.21 | -19.2 ± 4.0 |
| Sn | 948 | -6.38 | -6.73 ± 0.26 |
| Steel (304) | 1017 | -4.85 | -4.77 ± 0.25 |
| Ta | 1004 | -23.7 | -23.6 ± 0.25 |
| Th | 1511 | -18.0 | -11.9 ± 0.16 |
| Depleted U | 2435 | -12.44 | -5.11 ± 0.10 |
| $^{238}U$ | (998) | (-5.36) | -5.37 ± 0.25 |
| V | 527 | -0.95 | -1.80 ± 0.47 |
| W | 1867 | -18.66 | 10.0 ± 0.1 |
| Y | 582 | -2.32 | -4.0 ± 0.4 |
| Zr | 846 | -3.37 | -4.0 ± 0.3 |

[a]Excluding mass and worth of cladding or can. Accuracy ±0.25 Ih, but no better than 1% of value.

[b]Sample size: 1 x 2 x 2 in.

[c]Physicum I and II are mixtures of fission-product elements and their oxides. Compositions are given by Long et al. in Ref. 2.

[d]Sulfur samples (canned) obtained from different sources, suspected impurities in one or the other have not been resolved.

TABLE IV. Sample-size Effects in Measurements of Enriched-$B_4C$ Reactivity Coefficients

| Sample Space Dimensions, in. | Sample Dimensions, in. | Mass of Enriched $B_4C$,[a] g | Sample Worth, Ih[a] | Enriched-$B_4C$[a] Reactivity, Ih/kg | $^{10}B$ Reactivity Coefficients,[b] Ih/kg |
|---|---|---|---|---|---|
| 2 x 2 x 2 | 1/4 x 2 x 2 | 32.82 | -39.9 ± 0.3 | -1003 ± 9 | -1609 ± 15 |
| 2 x 2 x 2 | 1/2 x 2 x 2 | 63.97 | -60.5 ± 0.6 | -946 ± 9 | -1518 ± 15 |
| 2 x 2 x 2 | 3/4 x 2 x 2 | 96.21 | -85.8 ± 0.8 | -892 ± 9 | -1431 ± 14 |
| 2 x 2 x 2 | 1 x 2 x 2 | 128.16 | -110.0 ± 1.1 | -858 ± 9 | -1378 ± 14 |
| 2 x 2 x 2 | Four dispersed, each 1/4 x 2 x 2 | 128.16 | -117.5 ± 1.2 | -916 ± 9 | -1471 ± 15 |
| 1/4 x 2 x 2 | 1/4 x 2 x 2 | 31.49 | -33.2 ± 0.3 | -1056 ± 10 | -1695 ± 16 |
| 1/2 x 2 x 2 | 1/2 x 2 x 2 | 64.72 | -62.3 ± 0.6 | -963 ± 10 | -1545 ± 16 |
| 3/4 x 2 x 2 | 3/4 x 2 x 2 | 96.72 | -87.5 ± 0.9 | -905 ± 9 | -1452 ± 15 |
| 1 x 2 x 2 | 1 x 2 x 2 | 128.60 | -111.1 ± 1.1 | -864 ± 9 | -1388 ± 14 |

[a] $B_4C$ = 69.34 wt % B, B is 90.7 at. % $^{10}B$.
[b] Calculated using $B_4C$ = 62.32 wt % $^{10}B$ + 37.68 wt % $^{11}B$, carbon, and impurities, assuming $^{11}B$ and impurities of same worth as carbon (+1.3 Ih/kg).

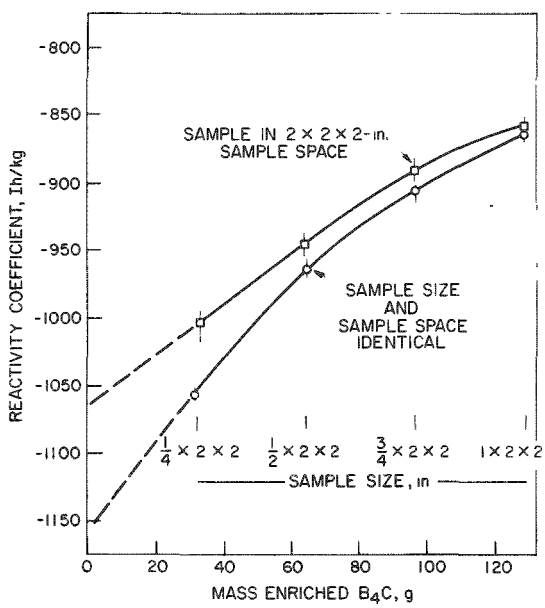


Fig. 14. Variation of $B_4C$ Reactivity Coefficient with Sample Size and Orientation

The results indicate a strong dependence of reactivity coefficient for a highly absorbent material like $B_4C$, according to the sample thickness used and also according to the medium in which the measurement is made. For comparison with perturbation theory, an extrapolated value at zero block thickness (infinite dilution) would be the most appropriate; a linear extension of the lower curve in Fig. 14 gives the value of -1146 Ih/kg of $B_4C$. The discrepancy for the smallest sample measured, a 1/4-in.-thick plate, thus amounts to -8%. Using a simple self-shielding formulation, the result indicates an average cross section for $^{10}B$ of 0.84 barn, which compares well with a value of 0.82 derived using the central spectrum from a diffusion-theory k calculation. This suggests that, to within the experimental accuracy, corrections for self-shielding in samples containing $^{10}B$ (or other highly absorbing materials with smoothly varying cross sections) can be either calculated or derived by extrapolation of results obtained using different sample sizes. However, the different coefficients obtained using the same samples in different sample-space configurations introduces considerable uncertainty about correlating the measurements against calculations using simple models for the sample and reactor environment.

## 2. Enriched-boron Experiments

Three different measurements of worth were made for highly enriched boron in the form of 1/8 x 2 x 2-in. steel-clad plates. Table V presents the details and results of these experiments. Although no appropriate extrapolation is feasible, appreciable self-shielding effects are again evident. Comparison between the derived worths of $^{10}B$ in Tables IV and V indicate that the presence of carbon in the $B_4C$ samples has negligible influence on the measurements.

TABLE V Sample-size Effects in Measurements of Enriched-boron Reactivity Coefficients at Core Center

| Sample-space Dimensions, in | Number of 1/8-in -thick Boron Plates in Sample[a] | Sample Content, g Boron Mixture[b] | Worth of Boron mixture,[b] Ih | $^{10}B$ Reactivity Coefficients,[c] Ih/kg |
|---|---|---|---|---|
| 2 x 2 x 2 | 10 | 39 5 | -53 8 ± 0 5 | -1575 ± 16 |
| 2 x 2 x 2 | 4 | 15 1 | -23 0 ± 0 3 | -1677 ± 22 |
| 1/2 x 2 x 2 | 4 | 15 1 | -22 0 ± 0 3 | -1686 ± 23 |

[a]Boron mixture in steel cladding, outside dimensions 1/8 x 2 x 2 in , plates dispersed in sample space with steel cans

[b]Mass and worth of steel in cans and spacers accounted for

[c]Mixture composition = 86 5 wt % $^{10}B$ + 13 5 wt % $^{11}B$ plus impurities, coefficients derived assuming $^{11}B$ and impurities of negligible worth

## 3. Tantalum Experiments

The tantalum was in the form of 1/8 x 2 x 2-in. plates. Worth measurements were made with the four plate/space combinations described in Table VI, with results as listed in the table. The self-shielding effects for this resonance-absorption material are less pronounced in the range of sample sizes involved than the effects with boron samples. However, even for the smallest tantalum sample, it is highly probable that the self-shielding of narrow resonances is extensive and the worth per kilogram for an infinitely dilute sample may be appreciably greater than the results given.

TABLE VI Sample-size Effects in Measurements of Tantalum Reactivity Coefficients at Core Center

| Sample-space Dimensions, in | Number of 1/8-in -thick Tantalum Plates in Sample | Mass of Tantalum, g | Sample Worth, Ih | Tantalum Reactivity Coefficients, Ih/kg |
|---|---|---|---|---|
| 1/2 x 2 x 2 | 4 | 524 | 12 0 ± 0 2 | -22 9 ± 0 4 |
| 2 x 2 x 2 | 4 dispersed | 524 | -12 8 ± 0 3 | -24 3 ± 0 6 |
| 2 x 2 x 2 | 2-in -cube can[a] | 1004 | -23 7 ± 0 3 | -23 6 ± 0 3 |
| 2 x 2 x 2 | 16 | 2102 | -44 4 ± 0 4 | -21 1 ± 0 2 |

[a]Powdered sample in steel can, effectively 50 vol % tantalum dispersed

### 4. Polyethylene Experiments

Plates of $CH_2$, 1/4 in. thick by 2 in. square, were dispersed in varying numbers with aluminum spacers within a 2 x 2 x 2-in. sample space at the core center. A measurement also was made with a $CH_2$-filled 1/2 x 2 x 2-in. space. Table VII gives the details and results of these worth experiments. As can be seen, the coefficients vary with no perceivable pattern. With this moderating material, proximity to fuel plates could be expected to have a strong influence on the worth, and the plate situations in the sample space are probably the cause of the erratic results. This indicates that one must assign a large uncertainty to measurements of $CH_2$ worths in some past ZPR-3 assemblies, and that there is a need for refinement in the experimental technique involving this material.

TABLE VII. Sample-size Effects in Measurements of Polyethylene Reactivity Coefficients at Core Center

| Sample-space Dimensions, in. | Number of 1/4-in.-thick $CH_2$ Plates in Sample | Mass of $CH_2$, g | $CH_2$ Worth, Ih | $CH_2$ Reactivity Coefficients, Ih/kg |
|---|---|---|---|---|
| 1/2 x 2 x 2 | 2 | 29.1 | 23.9 ± 0.3 | 820 ± 10 |
| 2 x 2 x 2 | 2 dispersed | 30.3 | 22.2 ± 0.3 | 731 ± 10 |
| 2 x 2 x 2 | 4 dispersed | 60.3 | 51.0 ± 0.5 | 845 ± 8 |
| 2 x 2 x 2 | 6 dispersed | 89.5 | 78.7 ± 0.8 | 880 ± 8 |
| 2 x 2 x 2 | 8 | 118.7 | 99.7 ± 1.0 | 840 ± 8 |

### 5. Depleted-uranium and Thorium Experiments

A comparison of the coefficients for thorium and depleted uranium in Tables II and III reveals similar agreement of worths between largely different sample sizes. However, there still may be appreciable differences from worths for infinitely dilute samples.

## D. Measurements of Material Worths at Edge of Core

Sample spaces at the core midplane near the core radial boundary were created by moving core material back from the front of drawers 1-J-12 and 2-V-20. These drawers had two sides adjacent to the core and two sides adjacent to the blanket. Reactivity coefficients were measured by successive material substitutions into the sample spaces, which were 1/4 x 2 x 2 in. for the high-reactivity fissile and capture samples and 1 x 2 x 2 in. for the lesser-worth materials. Tables VIII and IX present the results of the measurements in terms of the worths of the materials relative to void. No sample-size experiments were done in these locations.

TABLE VIII. Reactivity-coefficient Measurements for Fuel and Poison Materials at Radial Edge of Core

| Sample Material | Sample Dimensions, in. | Total Material Mass, g | Material Worth, Ih (±0.25) | Material Reactivity Coefficients, Ih/kg | Derived Isotopic Reactivity Coefficients | |
|---|---|---|---|---|---|---|
| | | | | | Isotope | Ih/kg |
| Enriched uranium[a] | 1/8 x 2 x 2 | 287.8 | 7.80 | 27.1 ± 0.9 | $^{235}U$ | 29.0 ± 0.9 |
| Depleted uranium[b] | 1 x 2 x 2 | 243.9 | 2.02 | 0.83 | $^{238}U$ | 0.77 ± 0.10 |
| Plutonium[a,c] | 1/4 x 2 x 2 | 186.0 | 8.10 | 43.6 ± 1.3 | $^{239}Pu$ | 45.4 ± 1.3[d] |
| Enriched $B_4C$[a,e] | 1/4 x 2 x 2 | 64.7 | -12.8 | -198 ± 4 | $^{10}B$ | -323 ± 4[f] |

[a]Placed in each of two 1/4 x 2 x 2-in. spaces; where needed, aluminum or steel spacers were used to fill volume.
[b]Placed in each of two 1 x 2 x 2-in. spaces.
[c]Composition specified in Table II
[d]Assuming $^{241}Pu$ equivalent to $^{239}Pu$, and $^{240}Pu$ worth/g = 0.2 x $^{239}Pu$ worth/g.
[e]As specified in Table IV.
[f]Calculated using 69.34 wt % boron, 30.66 wt % carbon + impurities, boron = 90.7 at. % $^{10}B$, assuming carbon, $^{11}B$, and impurities are worth 14.2 Ih/kg.

TABLE IX. Reactivity-coefficient Measurements in Two 1 x 2 x 2-in. Sample Spaces at Radial Edge of Core

| Sample Material | Total Sample Mass, g | Sample Worth, Ih (±0.25) | Material Reactivity Coefficients, Ih/kg |
|---|---|---|---|
| Al | 351 | 2.59 | 7.4 ± 0.7 |
| $Al_2O_3$ | 355 | 3.00 | 8.4 ± 0.7 |
| As | 382 | 0.27 | 0.7 ± 0.7 |
| Be | 241 | 3.63 | 15.1 ± 1.0 |
| Bi | 1276 | 3.00 | 2.35 ± 0.20 |
| C | 196.4 | 2.78 | 14.2 ± 1.3 |
| $CH_2$ | 59.5 | 7.95 | 134 ± 5 |
| Depleted U[a] | 2439 | 2.02 | 0.83 ± 0.10 |
| Fe | 1028 | 2.69 | 2.62 ± 0.24 |
| H[b] | (143.8) | (121.4) | 844 ± 2 |
| Mo | 1280 | 2.09 | 1.64 ± 0.20 |
| Na | 91.2 | 0.85 | 9.3 ± 2.7 |
| Nb | 490 | 1.14 | 2.33 ± 0.51 |
| Ni | 1504 | 3.52 | 3.06 ± 0.17 |
| O[c] | (471) | (4.53) | 9.6 ± 0.5 |
| Pb | 1475 | 3.45 | 2.34 ± 0.17 |
| S(ZPR-3)[d] | 199.8 | 0.99 | 4.96 ± 1.25 |
| S(ZPR-6)[d] | 63.1 | 0.32 | 5.1 ± 4.0 |
| Steel (304) | 1017 | 3.01 | 2.96 ± 0.25 |
| Th | 1511 | -0.18 | -0.12 |
| W | 1867 | 0.27 | 0.14 |

[a]0.206 wt % $^{235}U$.
[b]Inferred from carbon and $CH_2$ measurements.
[c]Inferred from Al and $Al_2O_3$ measurements.
[d]As defined in Table III.

# VI. MEASUREMENTS OF FISSION RATIOS AT CENTER OF CORE

## A. Scope of Measurements

Ratios of the fission rates of various isotopes at the center of the core constitute spectral indices which are characteristic of the core composition. Fission rates were measured with absolute fission chambers at the front of drawers 1-P-16 and 2-P-16 to obtain the indices for the Assembly 41 core; the ratios obtained should be similar to fission ratios measured in the other systems with the same 5/1 composition. Kirn counters,[5] the original parallel-plate chambers developed for ZPR-3 and used in all the past ZPR-3 assemblies, were used to obtain ratios of fissions in $^{233}U$, $^{234}U$, $^{236}U$, $^{238}U$, and $^{239}Pu$ to fissions in $^{235}U$. In addition, measurements of the $^{233}U/^{235}U$, $^{236}U/^{235}U$, and $^{238}U/^{235}U$ fission ratios were obtained with newer chambers of a lightweight construction, which perturbs the incident flux less than the Kirn design.

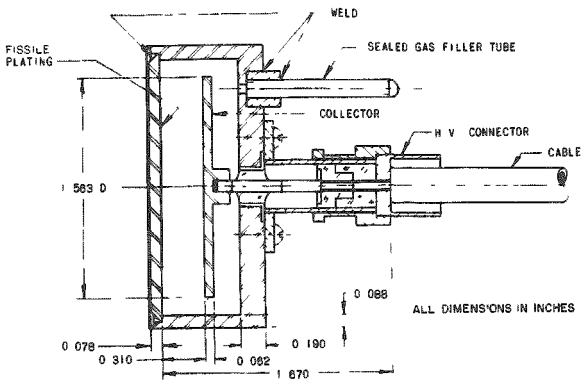


Fig. 15. Design of Kim Fission Chambers. ANL Neg. No. 103-A2154.

## B. Description of Fission Chambers

Figure 15 shows the construction of the absolute fission counters developed by Kirn.[5] The technique used for the original plating of a known amount of fissile material on the inside base of these counters has been discussed by Davey and Amundson,[6] who report on a reevaluation of the plating masses by a combination of intercalibrations in the thermal column and in the fast-flux beam hole of the Argonne Fast Source Reactor. Correction factors for the effect of inelastic scattering in the chamber walls are also given in Ref. 6. Table X gives the plating specifications for the Kirn counters involved in the Assembly 41 experiments.

Figure 16 shows the construction of the lightweight fission chambers which use the same basic parallel-plate scheme as the Kirn design but have thinner walls and use a continuous flow of gas. The fissile platings for these thin-wall chambers (designated TW) are on thin-steel foils, which are mounted into the bases of the chambers and are interchangeable. Plating masses and compositions for the foils used in Assembly 41 are included in Table X.

In the measurements, the pulses from each chamber preamplifier were amplified and input to discriminator circuits. Pulse-height settings were selected to discriminate out pulses of peak voltage less than that in the trough of the pulse-height distribution curve, thus eliminating gamma

events and an estimated 1-2% of the fission pulses. The reduction of the data involved the solution of simultaneous equations for several counter-pair count ratios to correct for minor isotope fissions and give isotopic fission ratios. Where necessary, the contributions of some minor constituents were estimated on the basis of calculations or other measurements.

TABLE X. Specifications of Platings in Fission Chambers

| Kirn Counter No. or Thin-wall-chamber Foil No. | Principal Isotope | Calibrated Plating Mass, μg | Plating Composition, wt % | | | | | |
|---|---|---|---|---|---|---|---|---|
| | | | $^{233}U$ | $^{234}U$ | $^{235}U$ | $^{236}U$ | $^{238}U$ | $^{239}Pu$ |
| Kirn No. 2 | $^{238}U$ | 499 ± 5 | - | - | 0.04 | - | 99.96 | - |
| Kirn No. 5 | $^{235}U$ | 804 | - | 1.07 | 93.41 | - | 5.52 | - |
| Kirn No. 11 | $^{234}U$ | 496 ± 10 | - | 94.02 | 4.29 | - | 1.69 | - |
| Kirn No. 18 | $^{233}U$ | 494 ± 10 | 98.33 | 0.13 | 0.01 | - | 1.53 | - |
| Kirn No. 21 | $^{239}Pu$ | 490 ± 6 | - | - | - | - | - | 99.97 |
| Kirn No. 24 | $^{236}U$ | 777 ± 9 | - | 0.06 | 2.85 | 96.48 | 0.62 | - |
| Foil No. 2 | $^{238}U$ | 495 ± 6 | - | - | 0.71 | - | 99.29 | - |
| Foil No. 3 | $^{235}U$ | 416 ± 4 | - | 1.04 | 93.22 | 0.28 | 5.46 | - |
| Foil No. 13B | $^{235}U$ | 435 ± 4 | - | 1.04 | 93.17 | 0.29 | 5.50 | - |
| Foil No. 14A | $^{238}U$ | 493 ± 5 | - | 0.006 | 0.72 | - | 99.27 | - |
| Foil No. 14B | $^{238}U$ | 493 ± 5 | - | 0.006 | 0.72 | - | 99.27 | - |
| Foil No. 21 | $^{233}U$ | 943 ± 12 | 98.33 | 0.127 | 0.01 | - | 1.53 | - |
| Foil No. 22 | $^{233}U$ | 946 ± 12 | 98.33 | 0.127 | 0.01 | - | 1.53 | - |
| Foil No. 23 | $^{233}U$ | 947 ± 12 | 98.33 | 0.127 | 0.01 | - | 1.53 | - |
| Foil No. 27 | $^{236}U$ | 397 ± 4 | - | 0.06 | 2.85 | 96.48 | 0.62 | - |
| Foil No. 28 | $^{236}U$ | 399 ± 4 | - | 0.06 | 2.85 | 96.48 | 0.62 | - |

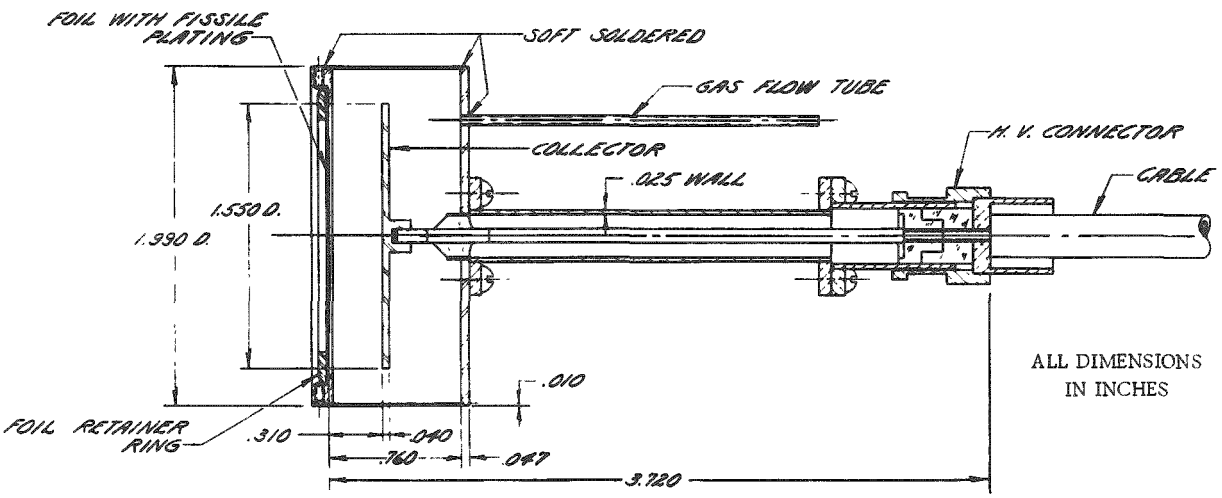


Fig. 16. Design of Thin-wall-steel, Gas-flow Fission Chambers. ANL Neg. No. 103-9200A.

## C. Details of Experimental Environment

Space was provided for the fission chambers at the core center by recessing the core materials $1\frac{1}{4}$ in. in drawers 1-P-16 and 2-P-16; small axial channels were constructed for the connecting leads. Figure 17 shows the material loadings in the vicinity of the central cavity during the measurements. During a run, the two chambers for obtaining a particular fission ratio were situated with their fissile platings back to back to expose the

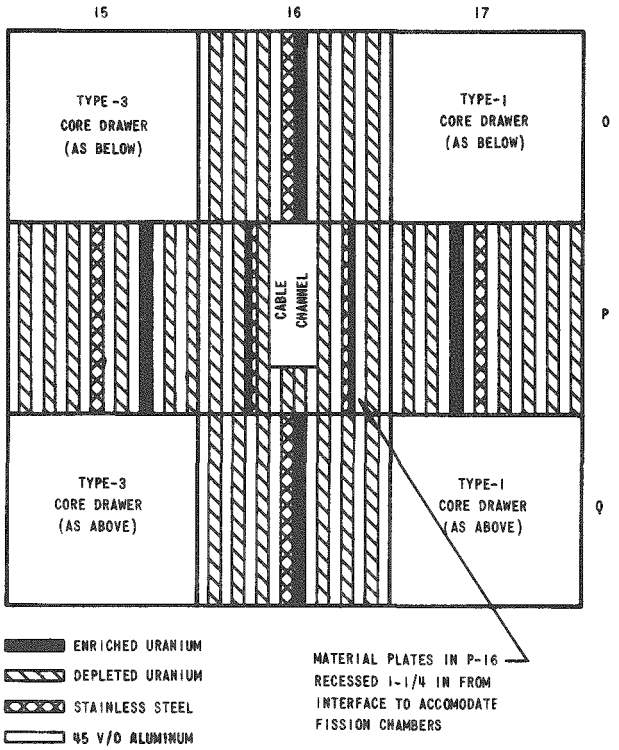


Fig. 17. Arrangement of Core Materials around Cavity for Fission-ratio Measurements

platings to an identical neutron flux. One feature of the environment that should be mentioned is that the loading of core materials behind the chambers in 1-P-16 and 2-P-16, and in the drawers above and below, represented one of the four types of loadings in the four-drawer sequence, having one full column of fuel per drawer. However, the proximity of the fuel in the side drawers (P-15 and P-17) should have enhanced the high-energy flux so that the overall spectrum incident on the foils was more nearly characteristic of the 1.25-columns-per-drawer fuel composition.

## D. Fission Ratios Measured with Kirn Counters

Table XI lists the pairs of Kirn counters placed at the center of the core, the measured ratio of counting rates, and the derived fission ratios for the counter principal isotopes. The final column of data gives the fission ratios corrected for wall-scattering effects using the factors given by Davey.[6] The probable errors given on the final values include the statistics of the measured chamber count ratios and the uncertainties in the calibrated masses.

TABLE XI. Fission-ratio Measurements at Center of Assembly 41 Using Kirn Counters

| Counter Pair in Central Cavity | | Ratio of Count Rates | Principal Isotopes, A/B | Derived Fission Ratios | Measured Fission Ratio with Wall-effect Correction |
|---|---|---|---|---|---|
| A | B | | | | |
| Kirn No. 18 | Kirn No. 5 | 0.9538 ± 0.0040 | $^{233}U/^{235}U$ | 1.469 ± 0.030 | 1.469 ± 0.030 |
| Kirn No. 11 | Kirn No. 5 | 0.2084 ± 0.0017 | $^{234}U/^{235}U$ | 0.290 ± 0.006 | 0.302 ± 0.007 |
| Kirn No. 24 | Kirn No. 5 | 0.1135 ± 0.0015 | $^{236}U/^{235}U$ | 0.0847 ± 0.0015 | 0.0898 ± 0.0017 |
| Kirn No. 2 | Kirn No. 5 | 0.02415 ± 0.00019 | $^{238}U/^{235}U$ | 0.0366 ± 0.0005 | 0.0395 ± 0.0006 |
| Kirn No. 21 | Kirn No. 5 | 0.7426 ± 0.0104 | $^{239}Pu/^{235}U$ | 1.164 ± 0.022 | 1.164 ± 0.022 |

## E. Fission Ratios Measured with Thin-wall Counters

Table XII gives the results of experiments with various $^{233}U$, $^{235}U$, $^{236}U$, and $^{238}U$ foils placed in pairs of thin-wall counters at the core center. This extensive series of measurements was in part a cross-calibration of foils of the same type of fissile material. Included in the table are some comparisons of Kirn and thin-wall counters containing platings of $^{235}U$ as the principal isotope.

TABLE XII. Fission-ratio Measurements at Center of Assembly 41 Using Thin-wall Gas-flow Chambers

| Chamber Pair at Core Center, Foil Number | | Ratio of Count Rates, A/B | Principal Isotopes, A/B | Derived Fission Ratio for Principal Isotopes |
|---|---|---|---|---|
| A | B | | | |
| TW, No. 21 | TW, No. 3 | 3.603 ± 0.041 | $^{233}U/^{235}U$ | 1.501 ± 0.029 |
| TW, No. 22 | TW, No. 3 | 3.684 ± 0.029 | $^{233}U/^{235}U$ | 1.531 ± 0.027 |
| TW, No. 23 | TW, No. 3 | 3.694 ± 0.015 | $^{233}U/^{235}U$ | 1.533 ± 0.025 |
| TW, No. 27 | TW, No. 3 | 0.1196 ± 0.0004 | $^{236}U/^{235}U$ | 0.0922 ± 0.0013 |
| TW, No. 28 | TW, No. 3 | 0.1213 ± 0.0006 | $^{236}U/^{235}U$ | 0.0932 ± 0.0014 |
| TW, No. 2 | TW, No. 3 | 0.05867 ± 0.00029 | $^{238}U/^{235}U$ | 0.0399 ± 0.0006 |
| TW, No. 14A | TW, No. 3 | 0.05817 ± 0.00035 | $^{238}U/^{235}U$ | 0.0396 ± 0.0006 |
| TW, No. 14B | TW, No. 3 | 0.05806 ± 0.0035 | $^{238}U/^{235}U$ | 0.0395 ± 0.0006 |
| TW, No. 13B | TW, No. 3 | 1.0443 ± 0.0094 | $^{235}U_{F_{13B}}/^{235}U_{F_3}$ | 0.999 ± 0.014 |
| Kirn, No. 5 | TW, No. 3 | 1.924 ± 0.023 | $^{235}U_{K_5}/^{235}U_{F_3}$ | 0.994 ±0.016 |

## F. Discussion of Results and Selection of Best Values

The numerous experiments cited in Table XII indicate the precision that can be assigned to ratios measured using chambers of this type and these methods of plating calibrations. Deviations of 2.5% are seen in results obtained with different $^{233}U$ foils. On the average, the dispersion of values for a particular type of plating is about ±1.5%. The last two measurements in Table XII show relatively good agreement of the intercalibration of $^{235}U$ foils for the thin-wall and Kirn chambers.

Comparisons of data in Tables XI and XII reveal some larger disagreements for particular fission ratios. The Kirn and thin-wall fission ratios of $^{238}U/^{235}U$ agree well, after correcting for wall scattering in the Kirn chamber. However, the Kirn-counter value for the $^{236}U/^{235}U$ ratio is about 3% lower than the ratios obtained with two different $^{236}U$ foils in thin-wall chambers. Also, the Kirn ratio for $^{233}U/^{235}U$ is about 4% lower than the values derived with the lighter-chamber foils. The $^{236}U$ and $^{233}U$ Kirn chambers used have since been involved in other intercalibrations of fission counters and have again shown larger than average deviations, and this is reflected in the uncertainties assigned to the calibrated masses for these counters in Table X. However, with the larger probable errors given, the Kirn $^{233}U/^{235}U$ and $^{236}U/^{235}U$ fission ratios are as valid as the measurements with the thin-wall chambers.

The best values for fission ratios have therefore been obtained as a weighted average of all the measurements given in Tables XI and XII; the weightings assigned were the inverse squares of the probable errors of the measurements. Table XIII gives these average values for the fission ratios compared with values calculated using ANL cross-section set 635 as reported by Davey.[3]

TABLE XIII. Average Fission Ratios Measured at Center of Assembly 41 Compared with Calculations

| Isotope Pair | Average Experimental Fission Ratio | Calculated Ratio[a] | C/E |
|---|---|---|---|
| $^{233}U/^{235}U$ | 1.512 ± 0.028 | 1.576 | 1.04 |
| $^{234}U/^{235}U$ | 0.302 ± 0.007 | 0.359 | 1.19 |
| $^{236}U/^{235}U$ | 0.0920 ± 0.0015 | 0.105 | 1.14 |
| $^{238}U/^{235}U$ | 0.0396 ± 0.0006 | 0.0437 | 1.10 |
| $^{239}Pu/^{235}U$ | 1.164 ± 0.022 | 1.228 | 1.05 |

[a]As reported by Davey,[3] using ANL cross-section set 635.

# VII. REACTION-RATE TRAVERSES THROUGH BASIC ASSEMBLY

The spatial and spectral variations of the neutron flux in ZPR-3 assemblies can be evaluated from measurements of reaction-rate profiles for reactions of various energy sensitivities, using the $^{235}U$ fission rate to characterize the general flux shapes, threshold-fission rates to determine high-energy flux shapes, and the $^{10}B(n,\alpha)$ reaction to obtain the low-energy flux distributions. In Assembly 41 these reaction-rate profiles were measured principally by traversing of small counters as described in Appendix D. Activations of uranium foils were also used.

This section describes the reaction-rate distributions measured in the normal Assembly 41 configuration, with depleted uranium blanketing the core radially and axially. Traverses through the assembly with other types of blanket are reported in Section IX.

## A. Axial Traverses through Core Center

Drawers 1-P-16 and 2-P-16 were each modified as shown in Fig. 18A to accommodate a 1/2-in.-dia traverse-guide tube along the reactor axis.

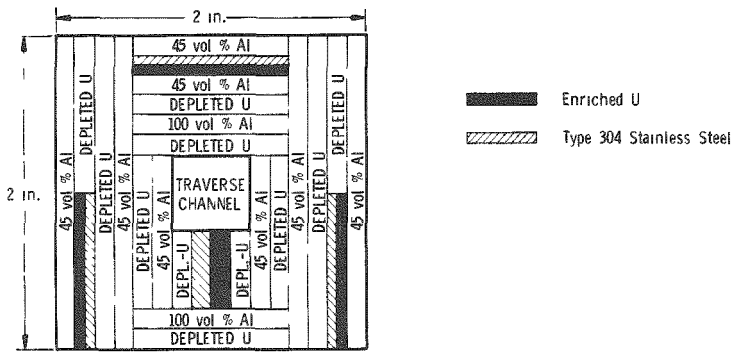


A. P-16 Drawer Loading (front view) for Axial Traverses

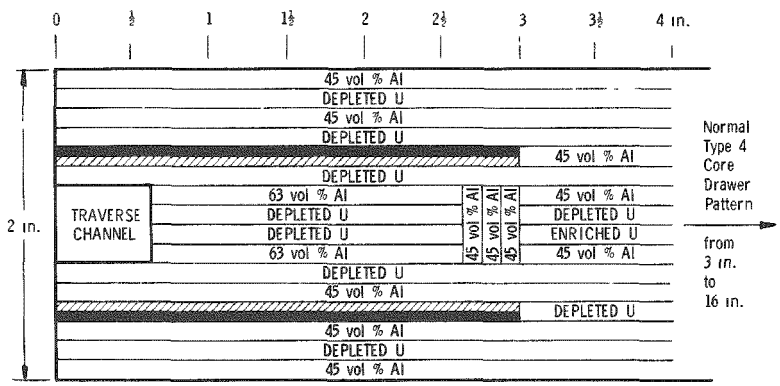


B. Loading of Column-16 Core Drawers for Radial Traverses

Fig. 18. Arrangements of Core Materials around Traverse Channels

Enriched-uranium and depleted-uranium fission counters and a $^{10}BF_3$ counter were traversed through the tube. Counting rates were obtained with each detector at several axial positions relative to the count rate of a fixed, standard detector. The results are presented in Table XIV as the fission or capture rate for the principal isotopes of the counters as percentages of the core-center rates. These results are shown graphically in Figs. 19-21.

TABLE XIV. Axial Reaction-rate Traverses through Center of Assembly 41 with Depleted-uranium Axial Blankets

| Axial Position, cm from core-center | Reaction Rate in Traverse along Core Axis in Drawers 1-P-16 and 2-P-16, % of core-center rate | | |
|---|---|---|---|
| | $^{235}U$ Fission (±1.5%) | $^{238}U$ Fission[a] | $^{10}B(n,\alpha)$ (±1.2%) |
| 0.00 | 100.0 | 100.0 | 100.0 |
| 2.54 | 100.9 | 100.6 | 100.8 |
| 5.08 | 98.9 | 99.4 | 99.4 |
| 10.16 | 97.1 | 97.6 | 97.2 |
| 20.32 | 84.8 | 86.7 | 85.3 |
| 30.48 | 69.7 | 67.3 | 69.3 |
| 35.56 | 59.9 | 54.8 | 61.5 |
| 38.10 | 53.8 | 45.7 | 57.8 |
| 40.64 | 47.3 | 34.2 | 48.6 |
| 43.18 | 40.5 | 20.5 | 41.8 |
| 45.72 | 33.3 | 12.7 | 35.1 |
| 50.80 | 22.4 | 5.1 | 23.9 |
| 60.96 | 8.79 | 1.04 | 10.6 |
| 68.58 | 3.54 | 0.36 | 4.86 |

[a]Accuracy estimated at ±5 in last significant figure or ±1.5%, whichever is larger.

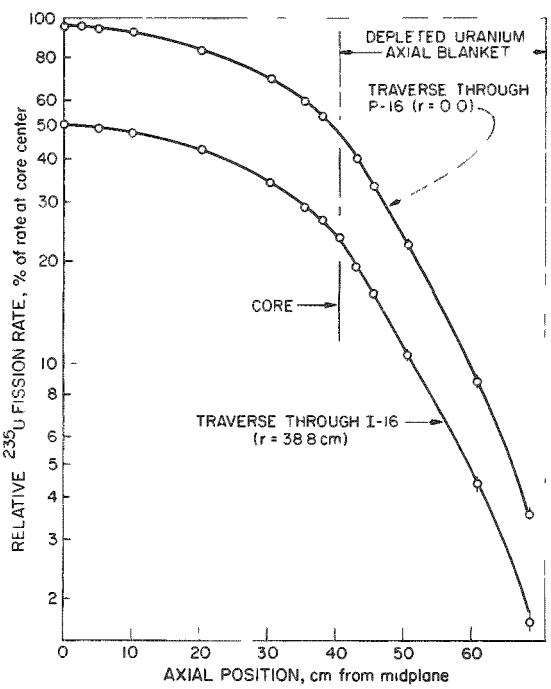


Fig. 19. Axial Fission-rate Profiles for $^{235}U$ in Assembly 41 with Depleted-uranium Blankets

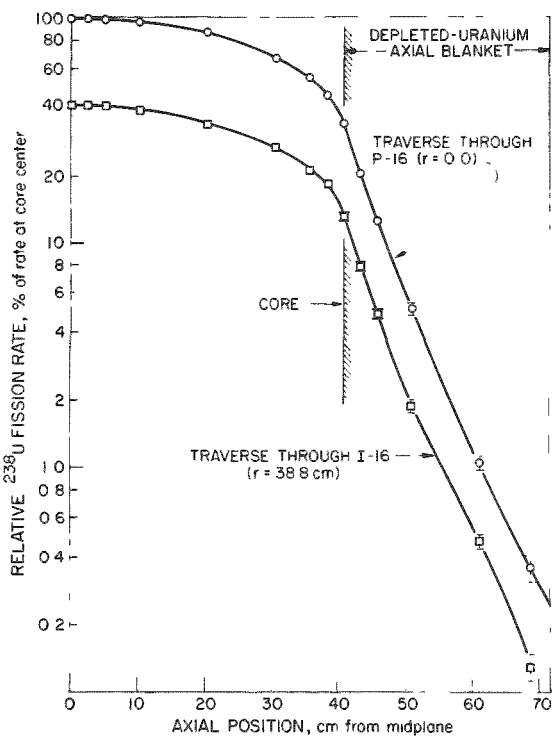


Fig. 20. Axial Fission-rate Profiles for $^{238}U$ in Assembly 41 with Depleted-uranium Blankets

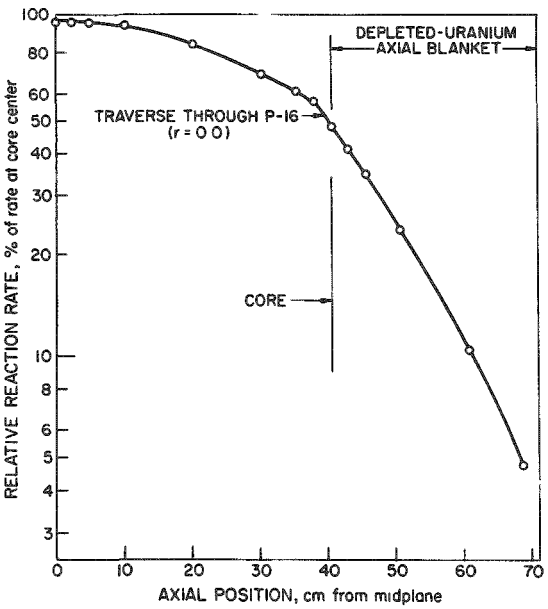


Fig. 21. Axial Reaction-rate Profile for $^{10}B$ in Assembly 41 with Depleted-uranium Blankets

## B. Axial Traverses at Radial Edge of Core

Drawers 1-I-16 and 2-I-16 were reloaded according to the pattern in Fig. 18A to allow traverses near the core radial boundary, parallel to the reactor axis. Only the uranium fission counters were used in these experiments, and the results are given in Table XV. The $^{235}U$ and $^{238}U$ axial fission profiles at the radial boundary are plotted with the axial profiles through the core center in Figs. 19 and 20. In each graph, the fission rates in the I-16 channel are given as percentages of the rate at the core center.

## C. Radial Traverses

The drawers and matrix tubes of column 16 in Half 2, from row C through row S, were reconstructed at the front to accommodate a guide tube for radial traverses at the core midplane. Figure 18B shows the rearrangement of the core drawers. The fronts of the blanket drawers (and the front of the blanket in the matrix) were similarly rearranged by using 1/8-in.-thick plates of depleted uranium. Count rates at several radii were obtained with the two uranium fission counters.

TABLE XV. Axial Reaction-rate Traverses at Core Radial Edge in Assembly 41 with Depleted-uranium Blankets

| Axial Position, cm from core midplane | Reaction Rate in Traverse Parallel to Core Axis in Drawers 1-I-16 and 2-I-16 (r = 38.8 cm), % of Rate at core midplane | |
|---|---|---|
| | $^{235}U$ Fission (±1.5%) | $^{238}U$ Fission[a] |
| 0.00 | 100.0 | 100.0 |
| 2.54 | 98.8 | 99.3 |
| 5.08 | 98.1 | 99.0 |
| 10.16 | 94.9 | 97.7 |
| 20.32 | 84.7 | 83.0 |
| 30.48 | 67.2 | 65.0 |
| 35.56 | 56.8 | 51.6 |
| 38.10 | 52.4 | 44.7 |
| 40.64 | 46.4 | 32.1 |
| 43.18 | 38.0 | 19.1 |
| 45.72 | 31.5 | 11.9 |
| 50.80 | 20.5 | 4.60 |
| 60.96 | 8.45 | 1.14 |
| 68.58 | 3.34 | 0.31 |

[a]Accuracy estimated at ±5 in last significant figure or ±1.5%, whichever is larger.

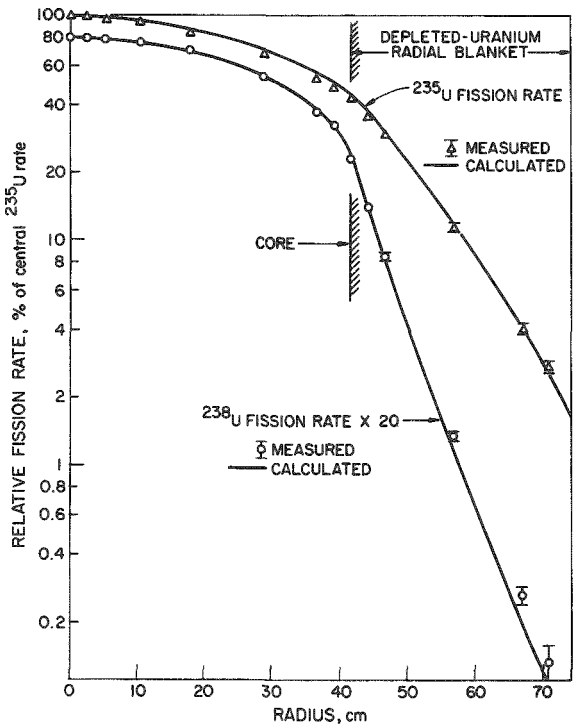


Fig. 22. Radial Fission-rate Profiles for $^{235}U$ and $^{238}U$ in Assembly 41 with Depleted-uranium Blankets

The results, reduced to relative fission rates versus radius for the counter constituents $^{235}U$ and $^{238}U$, are presented in Table XVI. Figure 22 shows the radial fission profiles for both isotopes at the reactor midplane compared with calculated profiles (see Section IX.D).

## D. Fine-flux Axial Traverse by Foil Irradiation

The data obtained in the axial counter traverse described in Section A above show some spurious variations in count rate near the core center. It appears, as it often has in past ZPR assemblies, that a significant flux depression might exist at the core center, presumably because of the discontinuity in the fuel columns presented by the machine interfaces. To investigate this further, a fine-flux traverse was obtained by irradiating thin foils of enriched uranium placed along the top of drawer 1-P-16. The results, presented in Fig. 23 as relative activation as a function of axial position, indicate no central flux depression within the 1% accuracy of the measurements. The foils in the experiment, however, spanned 2 in. across

TABLE XVI. Radial Reaction-rate Traverses at Midplane of Assembly 41 with Depleted-uranium Radial Blanket

| Radius, cm from core center | Relative Reaction Rate, % of core-center rate | |
|---|---|---|
| | $^{235}U$ Fission (±1.5%) | $^{238}U$ Fission[a] |
| 0.00 | 100.0 | 100.0 |
| 2.54 | 99.4 | 99.6 |
| 5.08 | 96.7 | 98.3 |
| 10.16 | 93.8 | 95.4 |
| 17.78 | 85.0 | 88.4 |
| 28.83 | 68.2 | 67.5 |
| 36.45 | 53.2 | 46.9 |
| 38.99 | 48.5 | 40.7 |
| 41.53 | 43.0 | 28.9 |
| 44.07 | 35.4 | 17.6 |
| 46.61 | 29.5 | 10.68 |
| 56.90 | 11.4 | 1.70 |
| 67.06 | 4.0 | 0.34 |
| 70.87 | 2.7 | 0.16 |

[a]Accuracy estimated at ±5 in last significant figure or ±1.5%, which is larger.

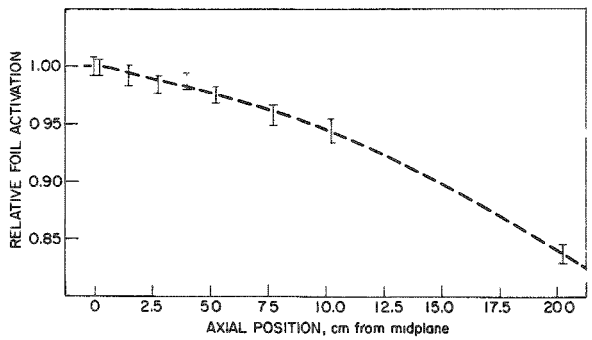


Fig. 23

Fine-flux Axial Traverse in Drawer 1-P-16
by Irradiation of Enriched-uranium Foils

the top of the drawer, and the activations obtained were averages over that span. Decreased central rates with the traverse counters might still result from using the loading of Fig. 18A in which a column of fuel ran adjacent to the traverse tube.

# VIII. ALUMINUM AND STEEL REFLECTOR EXPERIMENTS

Aluminum and steel were substituted for depleted uranium in portions of the axial and radial blankets to evaluate the relative reflective properties of these materials. Table XVII gives the average compositions of the regional loadings produced and designates labels for each type for reference in later tables and in the discussions below.

TABLE XVII. Compositions Involved in Experiments with Aluminum and Steel Reflectors

| Loading: | Uranium Axial Blanket[a] | Axial Spring Gap[b] | Half Al-Half U Blanket | Aluminum Axial Reflector | Half Steel-Half U Blanket | Steel Axial Reflector | Uranium Radial Blanket[c] | Aluminum Radial Reflector | Steel Radial Reflector |
|---|---|---|---|---|---|---|---|---|---|
| Designation: | UAB | Gap | Al/U | Al-AB | SS/U | SS-AB | URB | Al-RR | SS-RR |
| Composition, $10^{22}$ atoms/cm$^3$ | | | | | | | | | |
| $^{235}U$ | 0.0084 | - | 0.0042 | - | 0.0041 | - | 0.0084 | - | - |
| $^{238}U$ | 3.9962 | - | 1.9981 | - | 1.9749 | - | 3.9928 | - | - |
| Aluminum | - | - | 2.5078 | 5.0156 | - | - | - | 5.0284 | - |
| Iron | 0.5593 | 1.685 | 0.5593 | 0.5593 | 3.1873 | 5.7549 | 0.5049 | 0.5049 | 5.6919 |
| Chromium | 0.1391 | 0.419 | 0.1391 | 0.1391 | 0.7929 | 1.4316 | 0.1256 | 0.1256 | 1.4160 |
| Nickel | 0.0609 | 0.184 | 0.0609 | 0.0609 | 0.3470 | 0.6265 | 0.0550 | 0.0550 | 0.6196 |
| Manganese | 0.0058 | 0.018 | 0.0058 | 0.0058 | 0.0331 | 0.0598 | 0.0052 | 0.0052 | 0.0591 |
| Silicon | 0.0068 | 0.020 | 0.0068 | 0.0068 | 0.0388 | 0.0702 | 0.0062 | 0.0062 | 0.0615 |

[a]Regular axial-blanket drawer composition, excluding control drawers.
[b]0.66-cm gap in all axial blankets, situated from 53.42 to 54.08 cm from midplane of reactor.
[c]Average of inner- and outer-type radial blankets in three-row annulus.

## A. Aluminum in Axial Blanket

The 12-in.-long axial blanket in each assembly half was constructed from bricks of depleted uranium and extended 5 in. behind the core in the front drawers and 7 in. in the backup drawers (with a 0.3-in. spring gap between the two drawers). In the initial aluminum-reflector experiment, uranium was replaced with aluminum in alternate matrix positions in a radial wedge of the Half 1 axial blanket. The locations involved are indicated by the checkerboard pattern of Sector A in Fig. 24. The exchange (48.3 kg of aluminum for 340.2 kg of uranium) changed the Sector A average composition from that labeled UAB to the Al/U type in Table XVII and resulted in a 6.6-Ih loss in reactivity.

The aluminum-for-uranium substitution was then carried out in alternate locations of the remainder of the Half 1 axial blanket, in Sector B of Fig. 24 (excluding control drawers). A loss of 9.0 Ih was produced in exchanging 132 kg of aluminum for 931 kg of uranium, for changing Sector B from UAB to the Al/U composition.

With the entire Half 1 axial blanket a checkerboard mixture of uranium and aluminum (exclusive of control drawers), the uranium in the alternate locations of Sector A in Fig. 24 was then replaced with aluminum. The change, from type Al/U to type Al-AB in Sector A (while Sector B contained type Al/U), was worth -9.0 Ih.

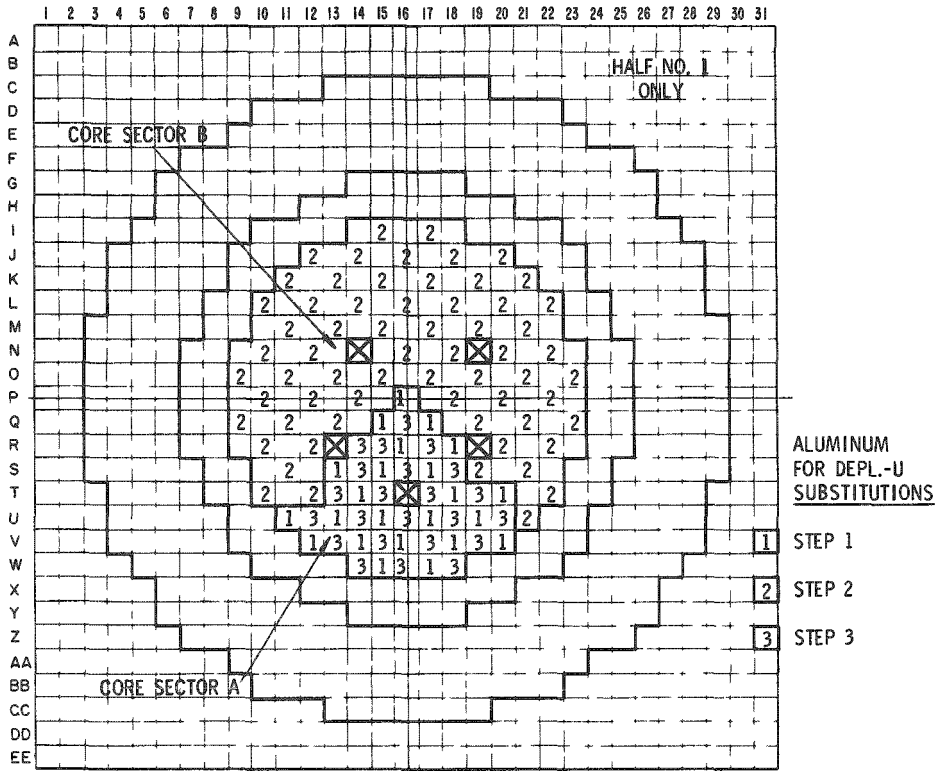


*Fig. 24. Locations for Aluminum-axial-reflector Experiments*

Part A of Table XVIII gives the pertinent details of the above experiments, and part B gives extrapolations of the results to the complete axial-blanket volume, including the control drawers not counted in the wedge sectors. It is seen that the worths in the experimental steps are not consistent with the net mass substitutions, indicating possible geometric perturbations and streaming effects. Therefore, the extrapolation for the worth of the full-density, full-volume aluminum reflectors in Table XVIII is highly uncertain.

B. Steel in Axial Blanket

Axial blankets composed of stainless steel were introduced directly after the experiments with aluminum. First, full-density steel was substituted for full-density aluminum in a 49-drawer wedge sector of the Half 1 blanket. Figure 25 shows the outline of the replacement region, Sector C, along with Sector D, which contained a checkerboard aluminum and uranium loading as constructed in previous experiments. The change of composition from type Al-AB to type SS-AB in Sector C, with type Al/U in Sector D, was worth +56.2 ± 0.3 Ih.

In the next step, alternate locations of the Sector C steel blanket were returned to a depleted-uranium loading, and the aluminum in Sector D was replaced with steel. This produced the checkerboard steel-and-uranium blanket pattern shown in Fig. 26 with the composition SS/U in Table XVII, and the change from the Fig. 25 configuration was worth +26.8 Ih.

TABLE XVIII. Worth of Aluminum Replacing Uranium in Axial Blanket

A. Experimental Results in Radial Sectors of Half No. 1 Axial Blanket

| Experimental Configuration | Composition of Sector A[a] in Fig. 24, Table XVII Designation[b] | Composition of Sector B[c] in Fig. 24, Table XVII Designation[b] | Relative Worth of Configuration, Ih |
|---|---|---|---|
| 1. Reference | UAB | UAB | 0 |
| 2. Half aluminum in Sector A | Al/U | UAB | -6.6 ± 0.2 |
| 3. Half aluminum in Sectors A and B | Al/U | Al/U | -15.6 ± 0.3 |
| 4. Full aluminum in Sector A | Al-AB | Al/U | -24.6 ± 0.3 |

B. Extrapolated Worths for Full Axial Blankets in Both Assembly Halves

| Blanket Type[d] | Composition Specification (table number and designation) | Relative Worth, Ih | Configuration (above) on Which Extrapolation Was Based |
|---|---|---|---|
| Normal depleted uranium | I: Average Axial Blanket | 0 | 1 |
| Alternate aluminum and uranium | XVII: Al/U | -32 ± 1 | 3 |
| Full-density aluminum | XVII: Al-AB | -80 ± 10 | 1 through 4 |

[a]Sector A excludes control drawer in 1-T-16.
[b]Specified composition loaded in front drawers from 40.72 to 53.42 cm, and in back drawers from 54.08 to 71.86 cm (axial distances from midplane). Spring gap between drawers.
[c]Sector B excludes control drawers.
[d]For full length of blankets, including spring gaps, behind 177 core drawers in each assembly half.

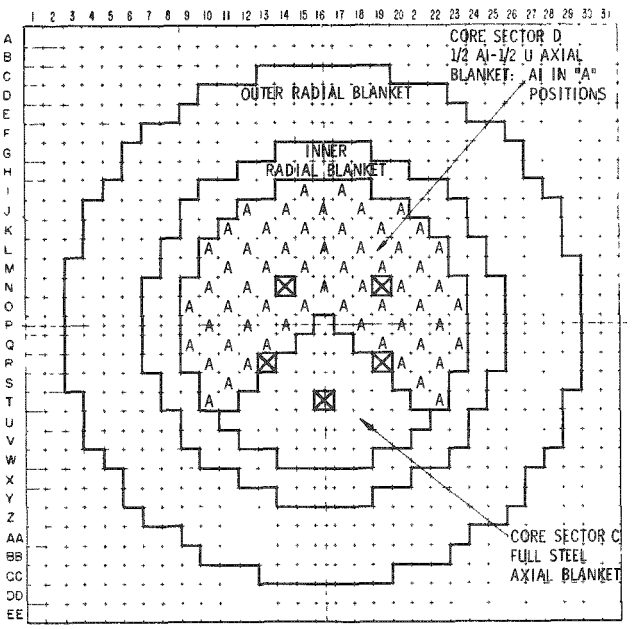


Fig. 25. Configuration of Half 1 Axial Blanket for Full-density Steel Reflector Experiment

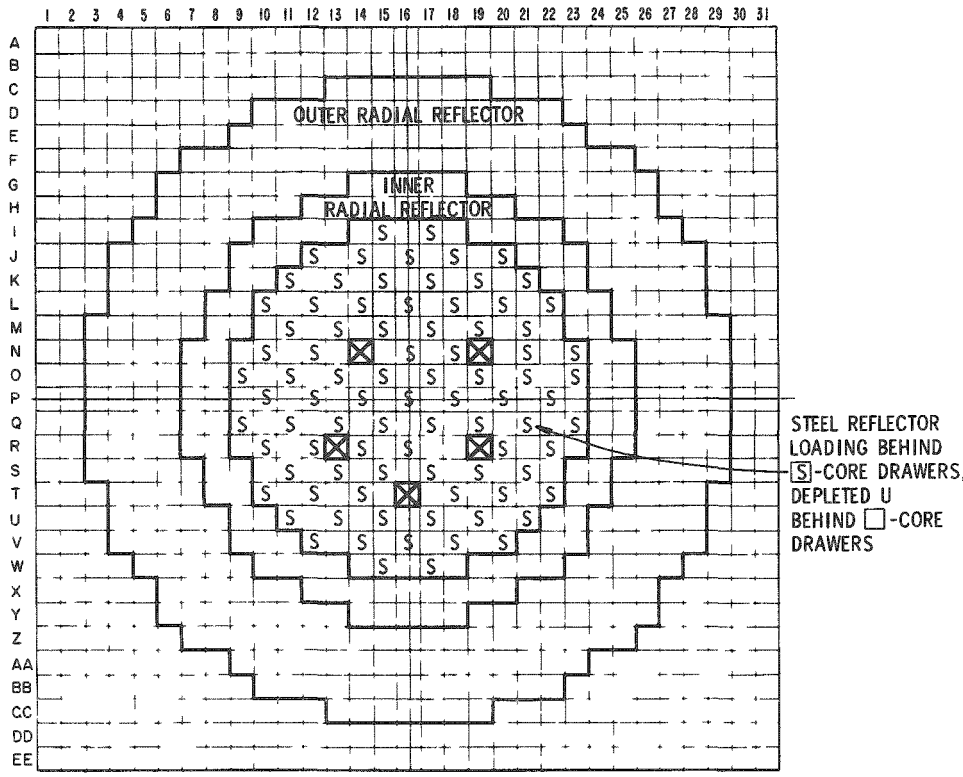


Fig. 26. Configuration of Half 1 Axial Blanket for Half-uranium, Half-steel Reflector Experiment

Part A of Table XIX gives the details of the two different loadings of steel in the axial blankets. The worths of these steel blankets are given as direct replacements of depleted-uranium blanket and were derived from the combined results of the steel and aluminum substitution experiments. Part B of the table gives estimated worths for substitutions of half-steel, half-uranium and full-steel-composition blankets for the normal depleted-uranium blankets on both ends of the core. The extrapolations again are assigned large uncertainties, due to the experimental technique.

## C. Aluminum Radial Reflectors

The worths of aluminum radial reflector shells relative to uranium blanket were measured at the radial boundary of one quadrant of the core in Half 1. Shell thicknesses of half-, one-, two-, and three-drawer units were constructed as indicated in Fig. 27. Aluminum was substituted for the depleted uranium in the radial blanket drawers to a depth of 16 in. (core half-length). The successive aluminum-reflector shell worths, measured relative to uranium blanket, were +1.9 Ih for the first half-drawer thickness, +0.2 Ih for the first full row of drawers, -6.7 Ih for the second row, and -9.0 Ih for the third row. These experiments are described in part A of Table XX in terms of total shell thicknesses and worths. In all cases, the blanket beyond the reflector shell was the regular depleted-uranium type to its normal outer boundary.

TABLE XIX. Worth of Steel Replacing Uranium in Axial Blanket

A. Experimental Results of Substitutions in Half No. 1 Blanket

| Experimental Configuration | Blanket Loading Description, Composition Designations as Defined in Table XVII | Relative Worth of Configuration, Ih |
|---|---|---|
| 1. Reference | Normal depleted-uranium composition, UAB, in 172-drawer axial blanket (excluding control drawers) | 0 |
| 5. Fig. 25 | Steel reflector, SS-AB, in 49-drawer Sector C<br>123-drawer Sector D (excluding control drawers) containing 60 aluminum and 63 uranium drawers in alternation--approximately the Al/U composition | +31.6 ± 0.4 |
| 6. Fig 26 | 172-drawer axial blanket containing 87 steel plus 85 uranium loadings, composition SS/U in Table XVII | +58.4 ± 0.6 |

B. Extrapolated Worths for Full Axial Blankets in Both Assembly Halves

| Blanket Type[a] | Composition Specification (table number and designation) | Relative Worth, Ih | Configuration on Which Extrapolation Was Based |
|---|---|---|---|
| Normal depleted uranium | I: Average Axial Blanket | 0 | |
| Alternate steel and uranium | XVII: SS/U | 120 ± 2 | 6 |
| Full-density steel | XVII: SS-AB | 250 ± 20 | 6, 5, 4[b] |

[a]Full 177-drawer blanket, with spring gaps, in each assembly half.
[b]Table XVIII.

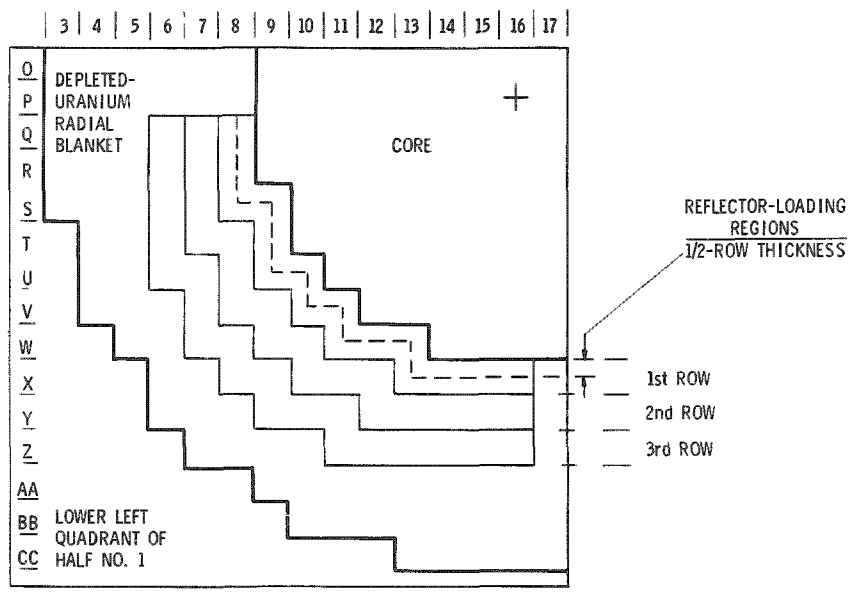


Fig. 27. Outline of Regions for Radial-reflector Experiments with Aluminum and Steel

TABLE XX. Worths of Aluminum Radial-reflector Annuli

A. Experimental Results in Quadrant of Half No. 1

| Annular Sector Specification[a] | | | | Worth of Aluminum Radial Reflector Replacing Uranium Radial Blanket, Ih (Al-RR for URB in Table XVII) | |
|---|---|---|---|---|---|
| Blanket Row | Inner Radius, cm | Outer Radius, cm | Volume, liters | Specified Row | Accumulated |
| 1st half | 41.60 | 45.09 | 9.74 | +1.9 ± 0.3 | +1.9 ± 0.3 |
| 1st full | 41.60 | 48.51 | 19.96 | +0.2 ± 0.3 | +0.2 ± 0.3 |
| 2nd full | 48.51 | 55.32 | 22.46 | -6.7 ± 0.3 | -6.5 ± 0.4 |
| 3rd full | 55.32 | 61.92 | 24.95 | -9.0 ± 0.5 | -15.5 ± 0.6 |

B. Extrapolated Worths of Full-circumferential Annular Reflectors of Aluminum

| Number of Matrix Rows in Annulus | Equivalent Reflector Thickness,[a] cm | Worth of Aluminum Reflector Replacing Uranium Blanket in Annulus,[b] Ih |
|---|---|---|
| 1/2 | 3.49 | +15.2 ± 2.4 |
| 1 | 6.91 | +1.8 ± 2.0 |
| 2 | 13.72 | -52 ± 3.0 |
| 3 | 20.32 | -124 ± 5.0 |

[a]As illustrated in Fig. 27; radii determined from quadrants of circles of equivalent area.

[b]Normal uranium blanket extending beyond reflector outer boundary to radius of 75 cm.

Part B of Table XX gives extrapolated worths of full-circumferential aluminum reflectors for the thicknesses used in the measurements. These extrapolation results are graphed in Fig. 28. A small, positive worth for replacement of uranium by aluminum is observed for small reflector thicknesses, but the worth turns negative as the number of aluminum rows is increased. This agrees with the positive worths of aluminum and uranium measured at the core edge and the negative worth of aluminum replacing uranium in the axial blanket.

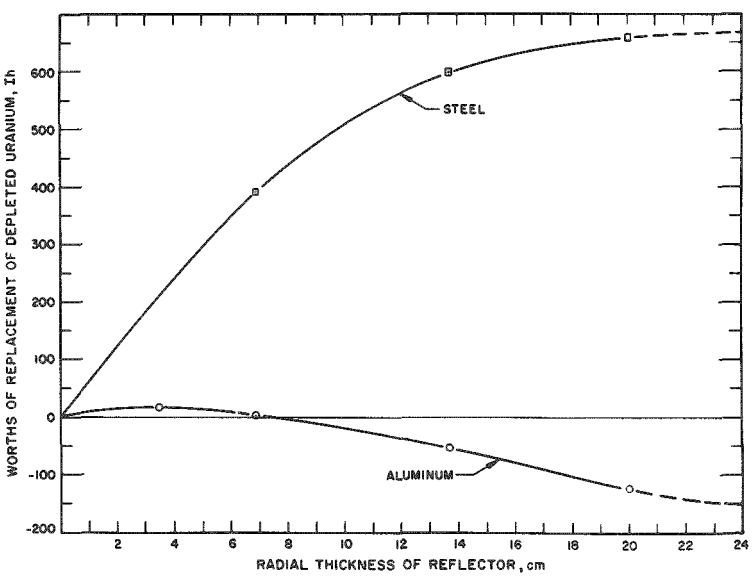


Fig. 28. Reactivity Worths of Steel and Aluminum Reflectors vs Thickness. ANL Neg. No. 103-2289.

## D. Steel Radial Reflectors

Steel reflector shells with thicknesses of one, two, and three drawers were constructed around one quadrant of the core in Half 1 in the same manner as in the aluminum reflector experiments (see Fig. 27). The reactivity worths of the successive rows of steel loading, relative to uranium blanket, were +48.7, +26.2, and +7.2 Ih. Table XXI presents these results as worths for the total-thickness configurations at the conclusion of each step.

TABLE XXI. Worths of Steel Radial-reflector Annuli

A. Experimental Results in Quadrant of Half No. 1

| Annular Sector Specification[a] | | | | Worth of Steel Radial Reflector Replacing Uranium Radial Blanket (SS-RR for URB in Table XVII) | |
|---|---|---|---|---|---|
| Blanket Row | Inner Radius, cm | Outer Radius, cm | Volume, liters | Specified Row | Accumulated |
| 1st | 41.60 | 48.51 | 19.96 | 48.7 ± 0.6 | 48.7 ± 0.6 |
| 2nd | 48.51 | 55.32 | 22.46 | 26.2 ± 0.4 | 74.9 ± 0.7 |
| 3rd | 55.32 | 61.92 | 24.95 | 7.2 ± 0.3 | 82.1 ± 0.8 |

B. Extrapolated Worths of Full-circumferential Annular Reflectors of Steel

| Number of Matrix Rows in Annulus | Equivalent Reflector Thickness,[a] cm | Worth of Steel Reflector Replacing Uranium Blanket in Annulus,[b] Ih |
|---|---|---|
| 1 | 6.91 | 390 ± 5 |
| 2 | 13.72 | 599 ± 6 |
| 3 | 20.32 | 657 ± 7 |

[a]As illustrated in Fig. 27; radii determined from quadrants of circles of equivalent area.
[b]Normal uranium blanket extending beyond reflector outer boundary to radius of 75 cm.

Table XXI also gives the extrapolated worths of one-, two-, and three-row steel-shell reflectors around the complete radial core boundary in both assembly halves, always with an outer radial blanket of uranium. Figure 28 includes a plot of the extrapolated steel-reflector worths.

# IX. EXPERIMENTS WITH PROTOTYPAL EBR-II RADIAL BLANKETS

Blanket compositions suitable for use in breeder reactors were substituted for the depleted uranium in a wedge sector of the Assembly 41 radial blanket. The experiments were concerned with methods of increasing the overall conversion rate of $^{238}U$ to plutonium or, conversely, decreasing the uranium inventory in breeder blankets. The approach taken was to introduce a moderator, such as carbon, in place of some of the $^{238}U$, thereby decreasing the $^{238}U$ density but also increasing the capture rate per atom.

## A. Blanket Types

The average composition of the radial and axial blankets in EBR-II[7] is about 45 vol % uranium, 20 vol % steel, and 35 vol % sodium. In the Assembly 41 experiments, three types of blanket configurations based on the EBR-II composition were studied in a 36° wedge sector of the radial blanket in both reactor halves. The blanket arrangements were:

1. A mockup of the EBR-II blanket with about 40 vol % uranium, 24 vol % steel, 25 vol % sodium, and 11 vol % void.

2. A simulated uranium carbide blanket with half the uranium in the type-1 composition replaced with graphite, giving approximately 20 vol % uranium, 20 vol % carbon, 24 vol % steel, 25 vol % sodium, and 11 vol % void.

3. A two-zone radial blanket in which the inner zone was the EBR-II type, as in arrangement 1 above, and the outer zone contained 40 vol % graphite instead of uranium.

Figure 29 presents front views of the drawer loadings used in these experiments, and Fig. 30 is an interface view of Half 1 showing the blanket wedge sector involved. In the two rows of blanket drawers near the core, the axial lengths of the blanket loadings were 16 in., identical to that of the core. Further out, the lengths of the blanket loadings were shorter by 1 in. in both assembly halves, a restriction imposed by the use of 15-in. drawers. The compositions and geometric specifications of these blanket loadings are presented in Table XXII.

## B. Blanket Replacements and Worths

The wedge-sector of the radial blanket as outlined in Fig. 30 contained 40 drawers out of the total of 400 for the blanket in each reactor half. Thus, the wedge extended an average angle of 36°. Assuming a direct extrapolation is valid, the relative worths of the different blanket types in the entire radial-blanket volume would be 10 times the corresponding worths in the wedge.

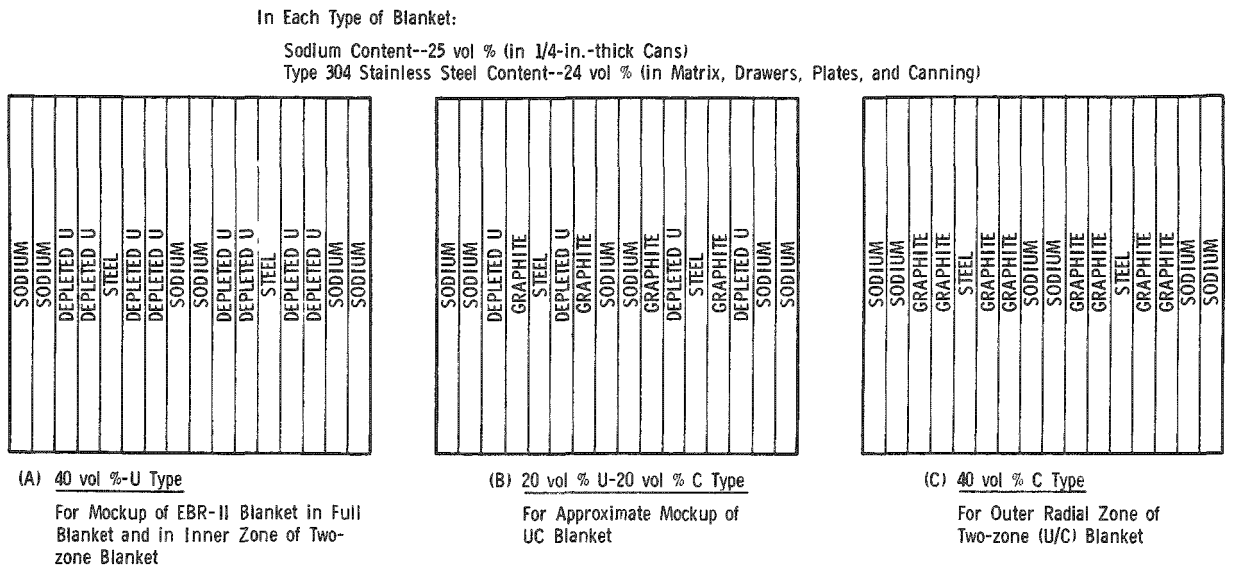


Fig. 29. Front Views of Radial-blanket Drawer Loadings for Experiments with Prototypal Breeder Blankets

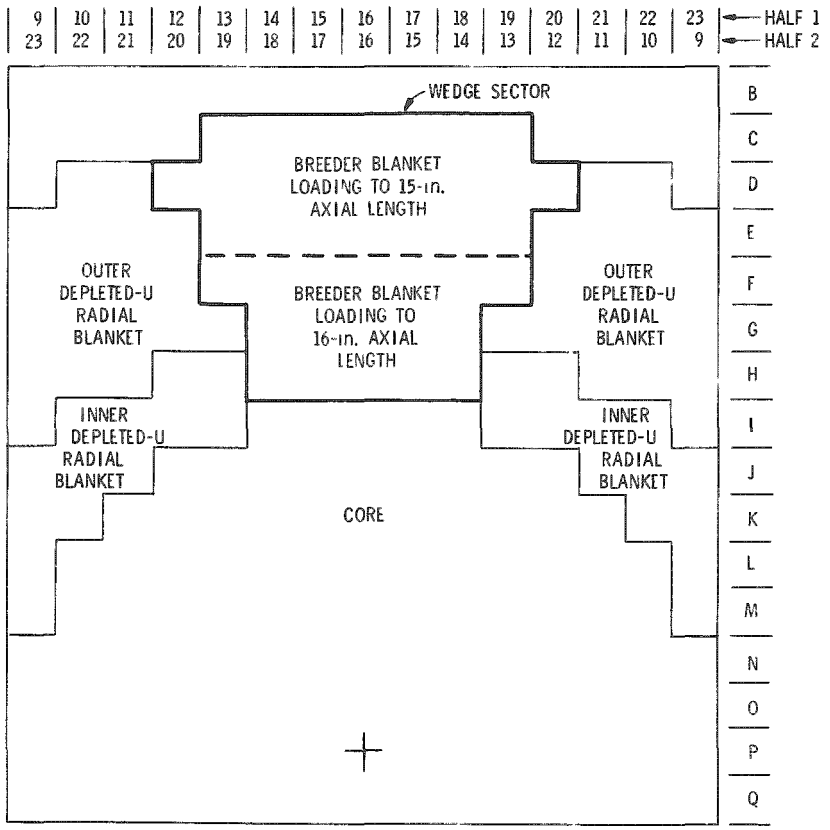


Fig. 30. Radial-blanket Wedge Sector in Both Assembly Halves for Experiments with Prototypal Breeder Blankets

TABLE XXII. Specifications for Breeder-blanket Experiments

| | Loading of 36° Wedge of Radial Blanket | | | | |
|---|---|---|---|---|---|
| | ZPR-3 Depleted U Blanket | EBR-II-type Blanket (40 vol % U) | UC-type Blanket (20 vol % U - 20 vol % C) | Two-zone Blanket | |
| | | | | Inner (40 vol % U) | Outer (40 vol % C) |
| Average Inner Radius, cm: | 41.55 | 41.55 | 41.55 | 41.55 | 58.18 |
| Average Outer Radius, cm: | 75.02 | 75.02 | 75.02 | 58.18 | 75.02 |
| Average Composition, $10^{22}$ atoms/cm$^3$ | | | | | |
| $^{235}$U | 0.0084 | 0.0040 | 0.0020 | 0.0040 | - |
| $^{238}$U | 3.9920 | 1.9366 | 0.9654 | 1.9288 | - |
| Iron | 0.4642 | 1.4603 | 1.4603 | 1.4553 | 1.4646 |
| Chromium | 0.1155 | 0.3633 | 0.3633 | 0.3620 | 0.3642 |
| Nickel | 0.0505 | 0.1590 | 0.1590 | 0.1584 | 0.1594 |
| Manganese | 0.0048 | 0.0152 | 0.0152 | 0.0151 | 0.0152 |
| Silicon | 0.0057 | 0.0178 | 0.0178 | 0.0177 | 0.0178 |
| Sodium | - | 0.6343 | 0.6343 | 0.6326 | 0.6354 |
| Carbon | - | - | 1.6588 | - | 3.3235 |

Replacement of the regular depleted-uranium radial blanket in the wedge by the simulated EBR-II blanket gave a reactivity loss of 25.8 ± 1 Ih. Changing from the EBR-II type to the UC-type blanket, by substituting graphite for half of the uranium, was worth -3.3 ± 0.8 Ih. Finally, the replacement of the UC-type blanket by the two-zone configuration in the wedge produced a loss of 2.9 ± 0.8 Ih. These results are presented in Table XXIII as the worths of full-circumferential blankets of the three breeder-type compositions relative to the normal Assembly 41 blanket composition. On the basis of these results, the three different breeder-blanket configurations would not entail significantly different critical core sizes in a fast breeder power reactor.

TABLE XXIII. Comparison of Worths of Prototypal Breeder-reactor Radial Blankets and ZPR-3 Blanket

| Composition Designation (as defined in Table XXII) | Relative Worth of Full Radial Blanket around Core of Assembly 41, Ih | |
|---|---|---|
| | Extrapolation from Experiments in 36° Wedge Sector[a] | Calculated by One-dimensional Diffusion Theory with Cross-section Set 635[b] |
| ZPR-3 Radial Blanket, 83 vol % Depleted U (reference loading) | 0 | 0 |
| EBR-II-type Breeder Blanket, 40 vol % U | -258 ± 10 | -201 |
| UC-type Breeder Blanket, 20 vol % U + 20 vol % C | -291 ± 10 | -219 |
| Two-zone Breeder Blanket: Inner 40 vol % U, Outer 40 vol % C | -320 ± 10 | -309 |

[a]Results of wedge-sector substitution have been multiplied by 10.
[b]Converted to inhours using 440 Ih/% k.

## C. Reaction-rate Profiles in Breeder Blankets

The $^{238}U$ capture rates were not actually measured in the different breeder blankets because of the extended irradiation that would have been required to obtain accurate radiochemical results. Instead, fission counters and a $BF_3$ counter were traversed through the blankets to obtain flux densities and spectral indices as functions of radius. The measured reaction-rate profiles could then be used to verify the flux profiles obtained from reactor calculations. The comparison of measured and calculated profiles would then approximately indicate the uncertainties in the $^{238}U$ capture rates and in the net breeding ratio derived from the calculations.

A traverse channel was constructed radially through the core and the blanket wedge sector in the same manner as described in Section VIII.C. The channel went through column 16; core drawers in the column were loaded as shown in Fig. 18B, and the drawer loadings shown in Fig. 31 were used to accommodate the traverse tube in the blanket regions. With each of the three blanket types installed in the sector, traverses were run with an enriched-uranium fission counter, a depleted-uranium fission counter, a $^{234}U$ fission counter, and a $^{10}BF_3$ proportional counter. Details of the counters are given in Appendix D. The traverse results, reduced to relative rates versus radius for fission in $^{235}U$, $^{238}U$, and $^{234}U$, and capture in $^{10}B$, are listed in Tables XXIV-XXVI.

## D. Comparison of Calculated and Experimental Reaction-rate Profiles

Radial distributions for the rates of $^{235}U$ fission, $^{238}U$ fission, $^{234}U$ fission, and $^{10}B$ capture were calculated using spatial flux distributions derived from k-effective calculations for the basic assembly and for configurations with the core surrounded by the three types of breeder blankets. A one-dimensional, diffusion-theory code was used with a 16-group cross-section set, ANL Set 635.[8] In the problems, zero-flux outer boundaries were stipulated on the basis of extrapolations of the measurements. The experimental and calculated reaction-rate profiles are compared in Figs. 32-35.

Figure 32 contains the $^{235}U$ fission-rate profiles. The poor correlations between calculation and measurement for the UC and two-zone blankets suggest that the cross sections used for carbon provided insufficient moderation.

The good correlation for the experimental and calculated $^{238}U$ fission rates versus radius, shown in Fig. 33, indicates that the high-energy flux is given adequately by the diffusion-theory calculations. Thus, the cross sections in the upper groups are sufficiently accurate for the blanket materials: $^{238}U$, carbon, sodium, and steel.

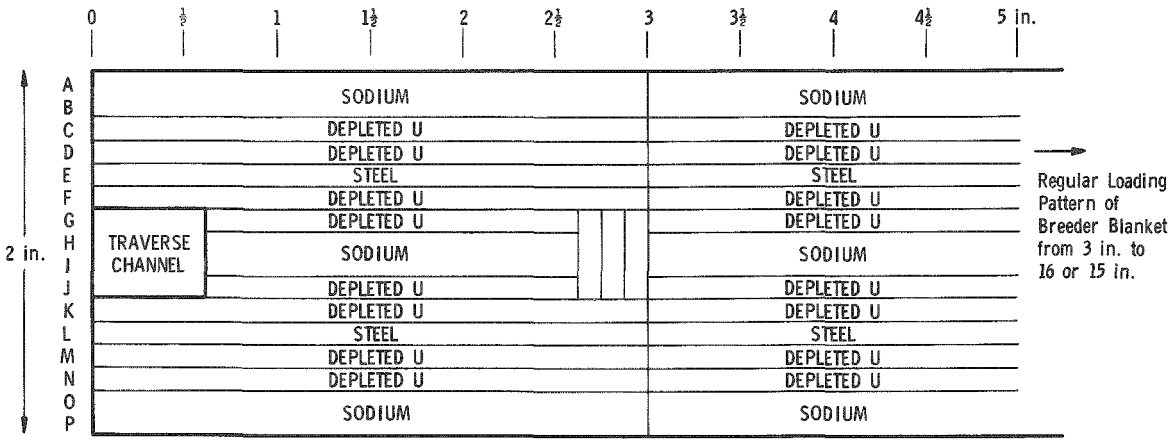


Figure shows drawer loading for traverses through EBR-II-type blanket (40 vol % U).

For traverses through UC-type blanket (20 vol % U-20 vol % C), depleted U shown in columns D, G, J, and M was replaced by graphite.

For traverses through two-zone blanket, inner-zone drawers were as in the figure, and outer-zone drawers had all depleted U replaced by graphite.

Fig. 31. Loadings of Matrix-column-16 Blanket Drawers for Radial Traverses through Prototypal Breeder Blankets

TABLE XXIV. Radial Reaction-rate Traverses through EBR-II-type Radial Blanket (40 vol % U)

| Radius, cm | $^{235}$U Fission[a] | $^{238}$U Fission[b] | $^{234}$U Fission[b] | $^{10}$B(n,$\alpha$)[c] |
|---|---|---|---|---|
| 0 | 100.0 | 100.0 | 100.0 | 100.0 |
| 2.54 | 99.2 | 99.4 | 99.6 | 99.4 |
| 5.08 | 98.3 | 96.4 | 97.5 | 98.0 |
| 10.16 | 96.4 | 95.3 | 93.4 | 93.4 |
| 17.78 | 86.5 | 86.5 | 86.3 | 83.5 |
| 28.83 | 68.6 | 65.8 | 64.6 | 65.7 |
| 36.45 | 54.0 | 47.6 | 47.5 | 48.9 |
| 39.00 | 48.3 | 39.7 | 41.4 | 43.7 |
| 41.53[d] | 43.3 | 29.3 | 32.5 | 38.2 |
| 44.07 | 37.8 | 19.1 ± 0.3 | 24.2 | 32.8 |
| 46.61 | 31.2 | 13.4 ± 0.3 | 18.5 | 28.5 |
| 54.36 | - | 4.51 ± 0.14 | 7.2 ±0.1 | 18.0 |
| 56.64 | 17.6 | - | - | - |
| 61.98 | 11.8 | 1.52 ± 0.08 | 3.2 ± 0.1 | 11.0 |
| 65.79 | 8.62 | - | - | - |
| 67.06 | - | 0.76 ± 0.06 | 1.85 ± 0.11 | 8.3 |
| 69.60 | 6.18 | - | - | - |
| 72.14 | 5.26 | 0.42 ± 0.04 | 1.04 ± 0.10 | 9.3 |
| 74.68 | 5.07 | - | - | - |

[a]Accuracy is ±0.9 or 1.5% of value, whichever is smaller.
[b]Unless specified, accuracy is ±1.2% of value.
[c]Accurary is ±1% of value.
[d]Radial boundary of core.

TABLE XXV. Radial Reaction-rate Traverses through UC-type Radial Blanket (20 vol % U + 20 vol % C)

| Radius, cm | $^{235}U$ Fission[a] | $^{238}U$ Fission[b] | $^{234}U$ Fission[c] | $^{10}B(n,\alpha)$[d] |
|---|---|---|---|---|
| 0 | 100.0 | 100.0 | 100.0 | 100.0 |
| 2.54 | 99.7 | 99.9 | 99.5 | 99.4 |
| 5.08 | 98.3 | 99.9 | 96.3 | 98.5 |
| 10.16 | 95.9 | 96.4 | 94.1 | 93.0 |
| 17.78 | 91.0 | 90.1 | 87.7 | 81.5 |
| 28.83 | 71.9 | 71.3 | 70.2 | 63.7 |
| 36.45 | 58.6 | 54.1 | 50.7 | 53.7 |
| 39.00 | 54.2 | 45.7 | 44.7 | 52.0 |
| 41.53[e] | 50.0 | 37.4 | 37.1 | 50.8 |
| 44.07 | 48.3 | 25.9 ± 0.4 | 27.9 | 52.8 |
| 46.61 | 46.0 | 18.0 ± 0.4 | 21.0 ± 0.4 | 51.8 |
| 54.36 | 35.3 | 6.8 ± 0.2 | 9.0 ± 0.3 | 43.1 |
| 61.98 | 24.7 | 2.4 ± 0.1 | 3.4 ± 0.2 | 31.8 |
| 67.06 | 17.3 | 1.30 ± 0.09 | 1.77 ± 0.15 | 24.8 |
| 72.14 | 11.3 | 0.85 ± 0.07 | 0.86 ± 0.25 | 22.2 |

[a]Accuracy is ±1.2% of value.
[b]Unless specified, accuracy is ±1.2% of value.
[c]Unless specified, accuracy is ±1.4% of value.
[d]Accuracy is ±1% of value.
[e]Radial boundary of core.

TABLE XXVI. Radial Reaction-rate Traverses through Two-zone Radial Blanket (Inner 40% U/Outer 40% C)

| Radius, cm | $^{235}U$ Fission[a] | $^{238}U$ Fission[b] | $^{234}U$ Fission[c] | $^{10}B(n,\alpha)$[a] |
|---|---|---|---|---|
| 0 | 100.0 | 100.0 | 100.0 | 100.0 |
| 2.54 | 99.6 | 97.4 | 99.8 | 99.4 |
| 5.08 | 99.2 | 96.3 | 98.5 | 97.2 |
| 10.16 | 96.7 | 94.8 | 93.2 | 91.5 |
| 17.78 | 88.8 | 84.5 | 84.6 | 83.4 |
| 28.83 | 68.8 | 66.8 | 66.0 | 64.8 |
| 36.45 | 54.8 | 47.5 | 49.1 | 50.0 |
| 39.00 | 49.2 | 39.8 | 40.9 | 45.1 |
| 41.53[d] | 44.8 | 28.0 | 32.8 | 41.2 |
| 44.07 | 39.2 | 18.6 | 24.9 | 37.2 |
| 46.61 | 35.4 | 12.7 ± 0.2 | 18.3 | 34.8 |
| 50.54 | 29.8 | - | - | 33.4 |
| 54.36 | 28.3 | 4.6 ± 0.1 | 8.0 ± 0.3 | 34.6 |
| 58.17[e] | 29.9 | - | - | 44.7 |
| 61.98 | 32.9 | 1.69 ± 0.08 | 2.2 ± 0.3 | 52.4 |
| 67.06 | 29.8 | 0.93 ± 0.06 | 0.8 ± 0.3 | 54.5 |
| 72.14 | 20.9 | 0.63 ± 0.05 | 0.5 ± 0.3 | 47.4 |

[a]Accuracy is ±1.2% of value.
[b]Unless specified, accuracy is ±1.2% of value.
[c]Unless specified, accuracy is ±1.3% of value.
[d]Core boundary.
[e]Boundary between inner- and outer-blanket zones.

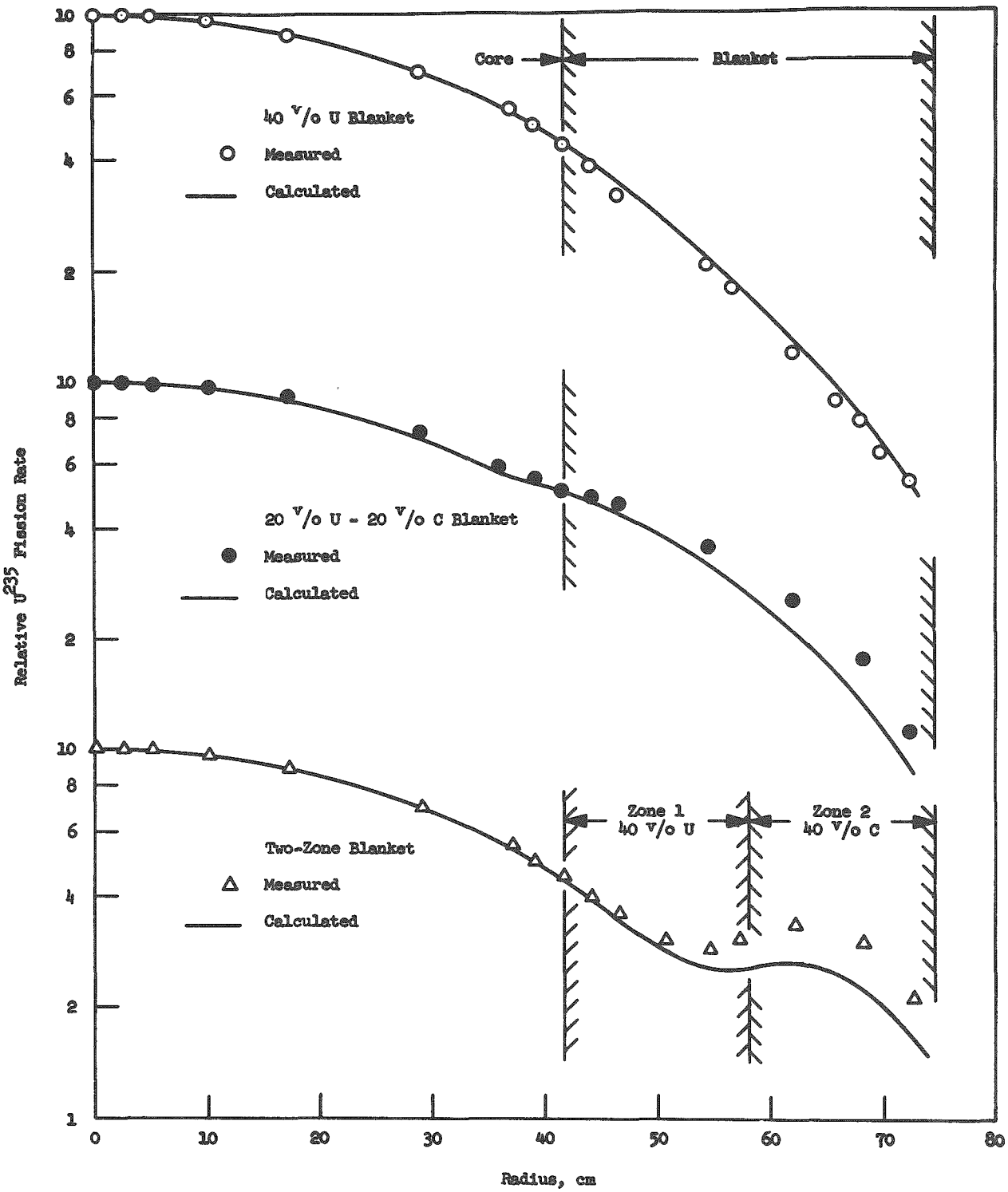


Fig. 32. Comparison of Measured and Calculated Radial Fission-rate Profiles for $^{235}U$ in Prototypal Breeder Blankets. ANL Neg. No. 103-2296.

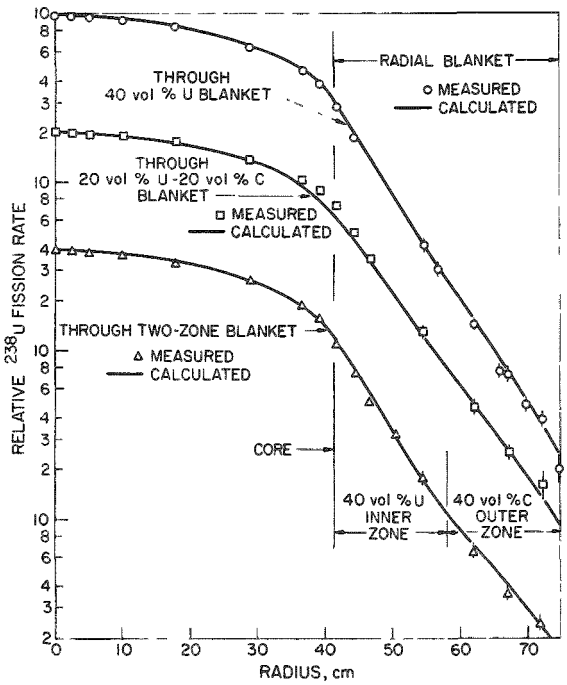


Fig. 33

Comparison of Measured and Calculated Radial Fission-rate Profiles for $^{238}U$ in Prototypal Breeder Blankets

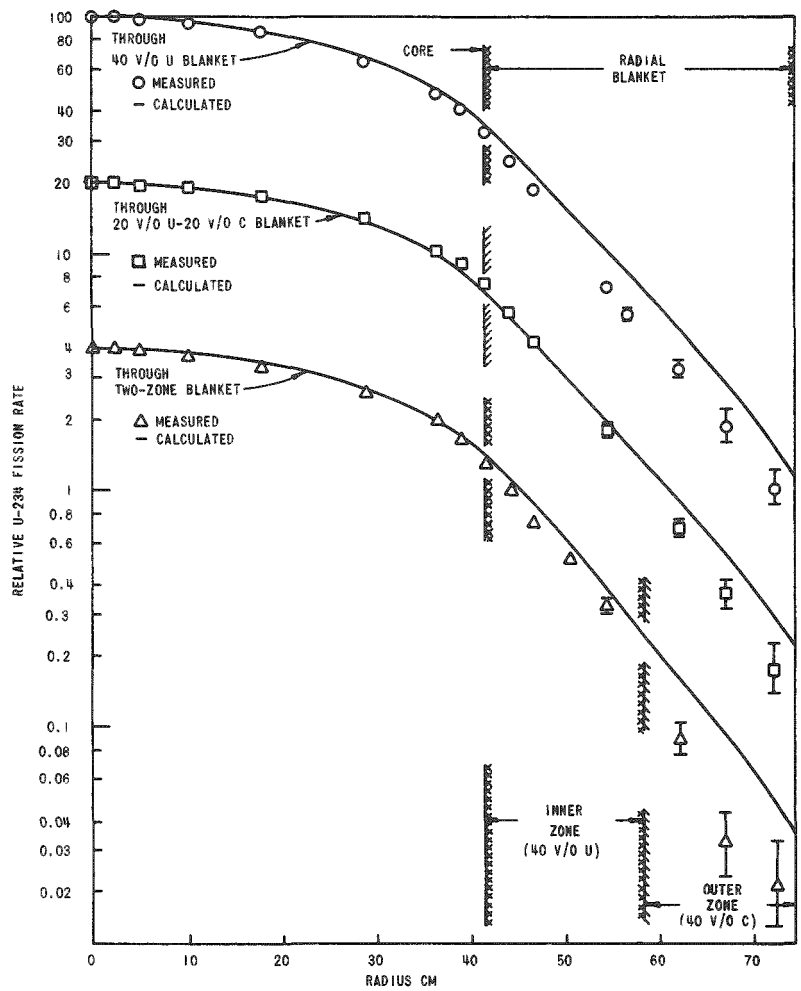


Fig. 34. Comparison of Measured and Calculated Radial Fission-rate Profiles for $^{234}U$ in Prototypal Breeder Blankets

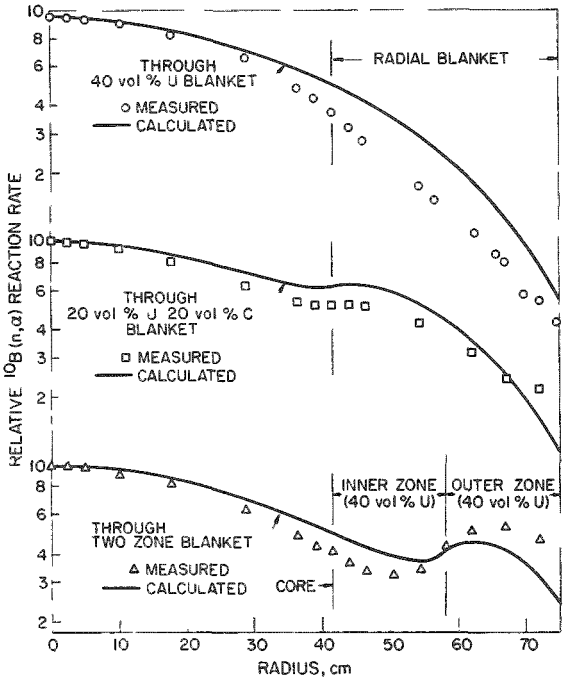


Fig. 35. Comparison of Measured and Calculated Radial Reaction-rate Profiles for $^{10}$B in Prototypal Breeder Blankets

Figure 34 shows that the calculated profiles for $^{234}$U fission are lower than the measurements in all three blanket configurations, but generally more so in the regions containing the 40 vol % uranium-type blanket. For this threshold reaction, it is not readily discernible which cross sections are to blame for the discrepancies; the group cross sections for $^{234}$U fission may be too high, or perhaps the $^{238}$U absorption is too low between the $^{234}$U and $^{238}$U fission threshold energies.

Figure 35 compares the experimental and calculated $^{10}$B capture rates versus radius. The poor correlation for this 1/v spectral index suggests several possible conclusions: (a) The capture and scattering cross sections of $^{238}$U in Set 635 provide excessive neutron flux in the low-energy region; (b) the carbon scattering cross sections are too low, giving insufficient moderation; (c) the variation with energy of the $^{10}$B(n,α) cross sections in Set 635 is distorted; and (d) the reactor model and boundary stipulations used are not appropriate for the low-energy flux. Of these, only conclusion b is substantiated by other reaction-rate traverses, the $^{235}$U fission-rate traverses compared with calculations in Fig. 32. It is also possible that the $BF_3$ counters registered excessive counting rates at the core center due to gamma sensitivity.

## E. Calculated $^{238}$U Capture Rates in Blankets

Figure 36 shows the calculated profiles for $^{238}$U capture in the three breeder-blanket configurations. Simple integration of the rate times concentration over the $^{238}$U-bearing regions gives the relative total capture rates of 1.00, 0.80, and 0.75 for the EBR-II-type, the UC-type, and two-zone blankets, respectively. As noted above, however, the cross-section set and possibly the calculational technique used provide spatial and spectral flux distributions that are not very accurate in the blankets. The closest approximation to the $^{238}$U capture profile would be

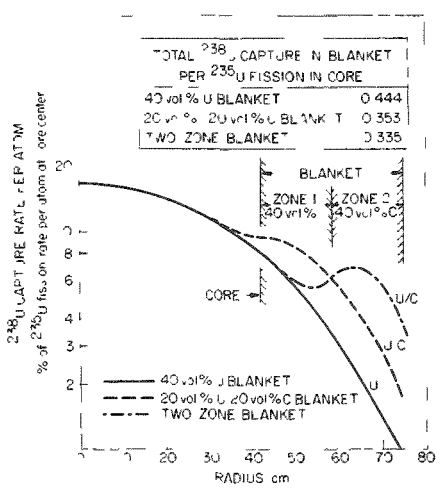


Fig. 36. Calculated Radial Capture-rate Profiles for $^{238}$U in Prototypal Breeder Blankets. ANL Neg. No 103-2297 Rev. 1.

the $^{235}U$ fission-rate profile; and the comparisons of calculated and measured $^{235}U$ fission rates suggest that the calculated $^{238}U$ capture rates are underestimated in the softer-spectrum, graphite-bearing blankets.

The conclusions possible from this series of experiments and calculations are only general. First, the technique used is not very reliable; accurate measurements of $^{238}U$ capture rates using foil irradiations or other methods are required for determining breeding-blanket performance. Second, the cross sections for carbon and $^{238}U$, possibly also sodium and steel, in Set 635 are improper for describing these blankets. Regarding the relative merits of the different types of breeder blankets, the experiments show that the introduction of moderation does increase the capture rate per unit mass in $^{238}U$ with no sacrifice in reactivity and possibly little sacrifice in overall breeding ratio.

# X. SIMULATED ROTARY-CONTROL-ROD EXPERIMENTS

A rotary-control-rod concept for fast reactors was investigated during the Assembly 41 program. The scheme prescribed a 6-in.-dia cylindrical rod, which would be located in the radial blanket just outside the core. The rod would be composed of blanket material, except for an eccentrically loaded section of enriched boron carbide. Reactivity control could thus be provided by rotating the poison section toward or away from the core. A suitable design for this concept would be that shown in Fig. 37, where the eccentric poison section is a 90° wedge sector of an outer, 1/2-in.-thick concentric shell. The magnitude of control offered by such a design was investigated in the Assembly 41 experiments in the regular depleted-uranium blanket and in the UC-type blanket described in Section IX.

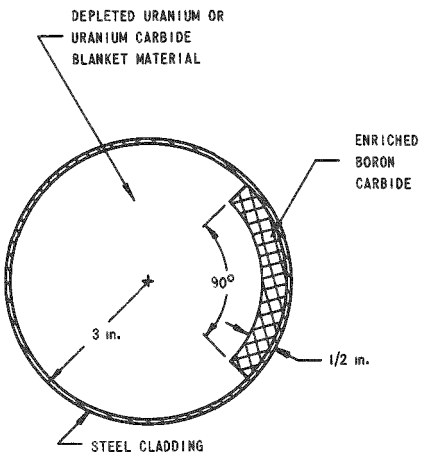


Fig. 37. Conceptual Design of a Rotary Control Rod for Use in the Radial Reflector of a Fast Reactor

An actual rotatable cylinder was not used for these measurements. Instead, the worths of boron carbide columns and blanket-material columns were determined at blanket locations representing the extreme-worth positions for the assumed rod design. A total thickness of 1/2 in. was used for the poison columns to obtain approximately the same self-shielding as in the reference design.

## A. Worth of $B_4C$ Rod in Depleted-uranium Blanket

The worth of a core-length "rod" of enriched boron carbide was measured at average distances of about 1/2 and 6 in. from the core in the normal Assembly 41 blanket. For the 1/2-in.-separation case, the rod consisted of two 1/4 x 2 x 16-in. columns of boron carbide positioned in the columns designated KIMN in drawer 1-P-8, as shown in Fig. 38. The same rod was positioned in locations CDEF of drawer 1-P-6 for the 6-in.-separation case.

At each rod position, the experiment proceeded in two steps. First, the four normal 2-in.-high columns of depleted uranium in the rod position were replaced with 1-in.-high columns of uranium with void above. Then the mockup $B_4C$ was substituted for the uranium and void, and the reactivity effect was determined from the change in critical positions of the ZPR-3 control rods. Table XXVII gives the details of these experiments, with the results expressed as material worths relative to void. To provide the desired information on rod reactivity, the results must then be expressed as worths of $B_4C$ displacing uranium. The latter worths, are, respectively, $-74.8 \pm 1$ and $-4.5 \pm 1$ Ih/kg for a column of $B_4C$ at the 1/2- and 6-in. separations from the core.

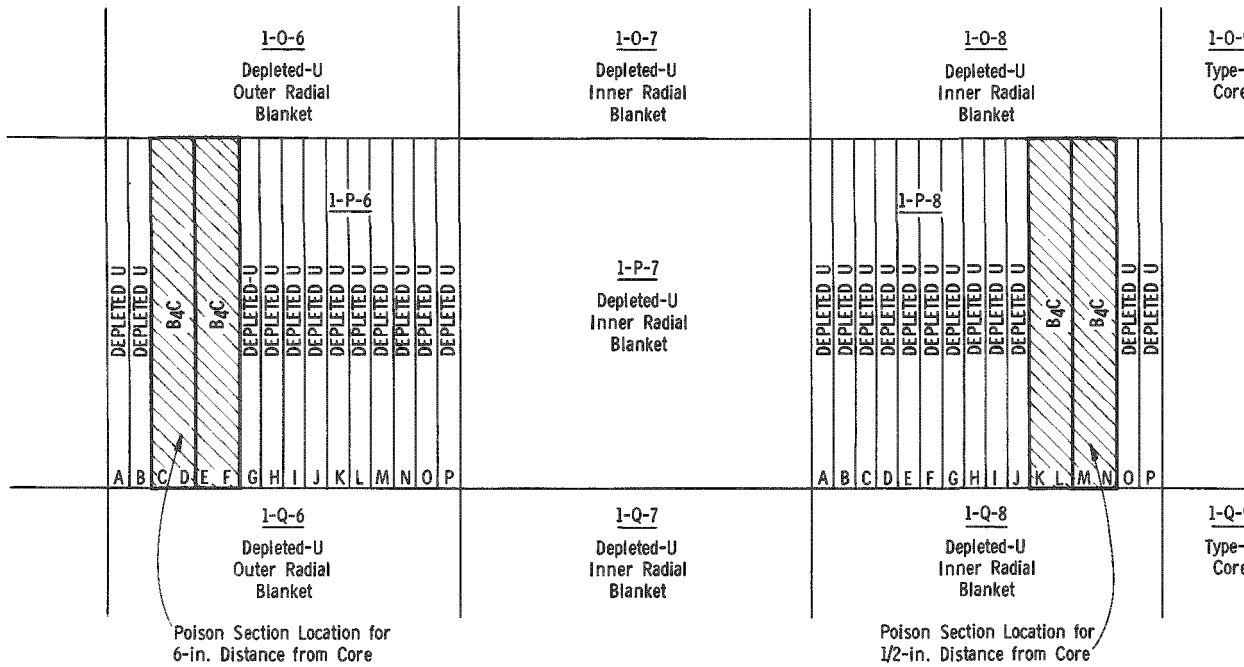


Fig. 38. Locations of $B_4C$ Loadings for Mockup Rotary-control-rod Experiments in Depleted-uranium Radial Blanket

TABLE XXVII. Enriched-$B_4C$ Substitution Experiments for Studies of Rotary-control-rod Worths in Depleted-uranium Blanket

| Substitution Specification[a] | | | | | | |
|---|---|---|---|---|---|---|
| Drawer | Column Locations | Average Distance from Core, in. | Width and Height of Replacement,[a] in. | Net Material[b] Replacement | Substitution Worth, Ih | Specific Material Worth over 16-in. Axial Length (relative to void) |
| 1-P-8 | KLMN | 0.59 | 1/2 x 1 | -2.353 kg U | -0.95 ± 0.2 | +0.404 ± 0.08 Ih/kg U |
| 1-P-8 | KLMN | 0.59 | 1/2 x 2 | -2.387 kg U<br>+0.518 kg $B_4C$ | -37.8 ± 0.4 | -71.1 ± 0.8 Ih/kg $B_4C$[c] |
| 1-P-6 | CDEF | 5.94 | 1/2 x 1 | -2.353 kg U | -0.15 ± 0.2 | +0.064 ± 0.08 Ih/kg U |
| 1-P-6 | CDEF | 5.94 | 1/2 x 2 | -2.387 kg U<br>+0.518 kg $B_4C$ | -2.2 ± 0.4 | -4.0 ± 0.8 Ih/kg $B_4C$ |

[a]Substitution for 16-in. axial length (half core height) in column positions as defined in Fig. 38.
[b]Uranium composition 0.206 wt % $^{235}U$; enriched $B_4C$ composition 69.34 wt % boron, with boron 90.7 at. % $^{10}B$.
[c]Derived after accounting for worth of displaced uranium.

The substitution results indicate a net reactivity change of 70 ± 2 Ih/kg of enriched boron carbide, in core-length sections, from oscillation between 1/2 and 6 in. from the core boundary. For the conceptual rotary-rod design in Fig. 37, with a $B_4C$ loading of about 2.2 kg, the possible reactivity control would thus be 157 Ih in a reactor like the one studied (i.e., having a 440-liter core surrounded by depleted-uranium blanket).

## B. Worth of $B_4C$ Rod in UC-type Blanket

The rotary-control-rod studies were also carried out in the wedge sector of UC blanket as constructed for the breeder-blanket experiments (see Section IX). In this blanket, the drawers involved were 2-F-16 and 2-H-16. Figure 39 shows the locations of the $B_4C$ substitutions. The replacement of the blanket material in the rod positions by the $B_4C$ columns proceeded similarly to the experiments described in Subsection A above. Table XXVIII presents the substitution details and the measured worths of blanket material and enriched $B_4C$ relative to void. For $B_4C$ replacing uranium, the worths are, respectively, -85.9 ± 1.0 and -12.4 ± 1 Ih/kg for a column of $B_4C$ at the 1/2- and 6-in. separations from the core.

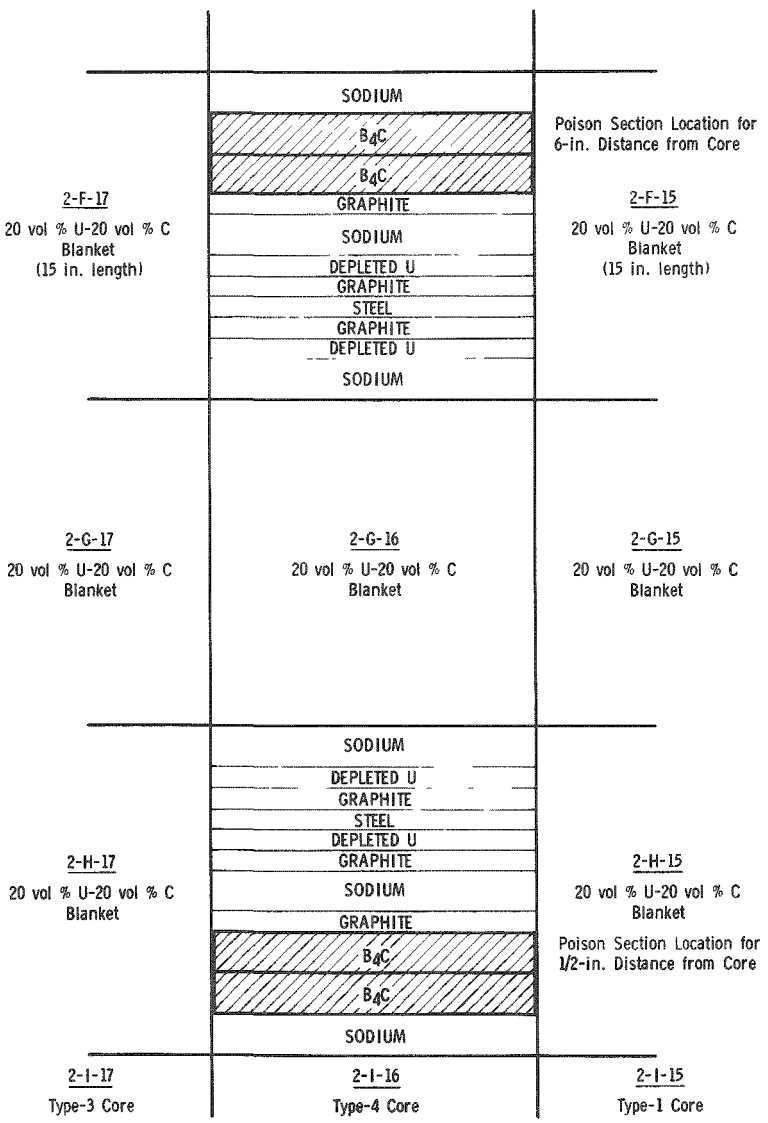


Fig. 39. Locations of $B_4C$ Loadings for Mockup Rotary-control-rod Experiments in UC-type Breeder Blanket

TABLE XXVIII. Enriched-$B_4C$ Substitution Experiments for Studies of Rotary-control-rod Worths in Prototypal Uranium Carbide Breeder Blanket

| Substitution Specification[a] | | | | | | |
|---|---|---|---|---|---|---|
| Drawer | Column Locations (from bottom of drawer), in. | Average Distance from Core, in. | Height and Width of Replacement, in. | Net Material[b] Replacement | Substitution Worth, Ih | Specific Material Worth over 16-in. Axial Length (relative to void) |
| 2-H-16 | 1/4 to 3/4 | 0.59 | 1/2 x 1 | -1.49 kg blanket | -1.55 ± 0.2 | +1.04 ± 0.13 Ih/kg blanket |
| 2-H-16 | 1/4 to 3/4 | 0.59 | 1/2 x 1 | +0.260 kg $B_4C$[d] | -23.2 ± 0.4 | -89 ± 2 Ih/kg $B_4C$ |
| 2-H-16 | 1/4 to 3/4 | 0.59 | 1/2 x 2 | -2.98 kg blanket +0.519 kg $B_4C$[d] | -44.6 ± 0.4 | -96 ± 1 Ih/kg $B_4C$[c] |
| 2-F-16 | 1-1/4 to 1-3/4 | 5.94 | 1/2 x 1 | -1.49 kg blanket | -0.40 ± 0.2 | +0.27 ± 0.15 Ih/kg blanket |
| 2-F-16 | 1-1/4 to 1-3/4 | 5.94 | 1/2 x 2 | -1.49 kg blanket +0.519 kg $B_4C$[d] | -6.45 ± 0.4 | -11 ± 1 Ih/kg $B_4C$[c] |

[a] 16-in. axial extension (half core height) in column positions as shown in Fig. 39.
[b] Blanket material replaced consisted of 79.87 wt % depleted uranium, 3.47 wt % carbon, 16.66 wt % steel.
[c] Derived after accounting for worth of displaced blanket.
[d] Enriched $B_4C$ composition 69.34 wt % boron, with boron 90.7 at. % $^{10}B$.

The net worth of transferring the poison section between 1/2 and 6 in. from the core amounts to 73.5 ± 1.5 Ih/kg of $B_4C$. Thus, with a rotary rod of the Fig. 37 design in a UC-type blanket around a 440-liter core, approximately 162 Ih of reactivity control could be expected.

The net reactivity control offered by the rotary-rod design was thus found to be almost identical in the regular depleted-uranium and the UC-type blankets. As would be expected from the moderated spectrum, the $B_4C$ worth at specific locations was higher with the UC-type blanket than with the regular depleted-uranium blanket. However, the difference in worth of the poison between "in" and "out" positions was the same in both blankets.

# XI. ASSEMBLY 41 RESULTS COMPARED WITH RELEVANT MEASUREMENTS IN A FAST EXPONENTIAL EXPERIMENT WITH $^{238}U/^{235}U$ RATIO OF 5/1

## A. Details of the Exponential Experiment

A 5/1 uranium composition similar to that of the Assembly 41 core had been investigated as a fast exponential experiment in 1955.[9] Figure 40 is a diagram of this experiment. The neutron source for the fast pile was Argonne's ZPR-4, a water-moderated, thermal critical facility. Between the source reactor and the fast system was an 8-in.-thick block of natural uranium, called the pedestal, serving as a thermal-neutron filter. The fast pile rested on a 12-in.-thick reflector constructed variously from blocks of one of the following: natural uranium, iron, aluminum, or lead. Geometric bucklings were obtained from flux traverses through the pile center in the three axial directions; these values then provided the material buckling of the 5/1 composition. With each different reflector in place, the reflector savings was determined as the displacement of the Z-axis flux peak from the pile center.

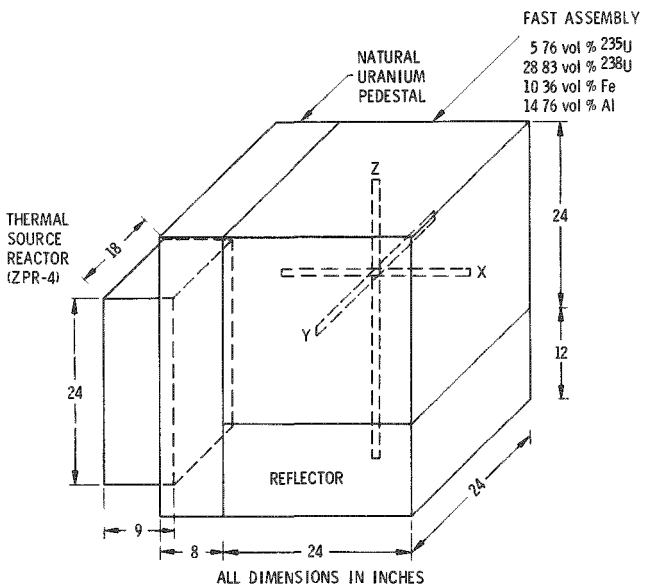


Fig. 40. 5/1 Fast Exponential Experiment. ANL Neg. No. 103-2287.

Small fission chambers were used to obtain the flux profiles; the fission ratios indicated an acceptable zone of spectral equilibrium. However, subsequent studies[10] indicated that a true spectral equilibrium, representative of the asymptotic spectrum for the pile composition, may not have been attained in the experiments throughout the regions of the buckling measurements. In addition, the studies suggested that excessive neutron leakage into the reflectors directly from the source reactor could give erroneous reflector savings.

Table XXIX compares the 5/1 pile composition with that of the core of Assembly 41. The pile had slightly less $^{235}U$ density and about 4 vol % less iron and aluminum. On the basis of other exponential experiments cited in Ref. 9 with different aluminum and $^{235}U$ densities, the core characteristics of Assembly 41 should differ by less than 10% from those in the related exponential pile.

TABLE XXIX. Comparison of Compositions and Results of Fast Exponential Experiment and Assembly 41

| Parameter | 5/1 Fast Exponential | | Assembly 41 | |
|---|---|---|---|---|
| Pile or Core Composition, vol % | | | | |
| $^{235}U$ | 5.76 | | 5.96 | |
| $^{238}U$ | 28.83 | | 29.00 | |
| Iron or steel | 10.36 iron | | 14.00 steel | |
| Aluminum | 14.76 | | 18.00 | |
| Void | 39.77 | | 33.00 | |
| Measured Root Buckling, $cm^{-1}$ | 0.0404 ± 0.0002 | | 0.0503 ± 0.0020 | |
| Reflector Savings, cm | | | | |
| Uranium | 100 vol % natural U: | 27.7 ± 2.0 | 83 vol % depleted U, 9 vol % steel: | 20.6 ± 1 |
| Iron | 100 vol % Fe: | 30.0 ± 3.0 | 93 vol % steel: | 22.8 ± 1 |
| Aluminum | 100 vol % Al: | 30.5 ± 3.0 | 83 vol % Al, 9 vol % steel: | 19.9 ± 1 |
| Fission Ratio, $^{235}U/^{238}U$ | 26.0 ± 0.5 | | 25.1 ± 0.5 | |

## B. Comparison of Characteristics of Assembly 41 and 5/1 Fast Exponential Experiment

The exponential experiment involved relatively few measurements: material buckling, reflector savings, and fission ratios. These are included in Table XXIX, along with values derived from results in Assembly 41. A buckling for Assembly 41 was obtained from cosine and Bessel-function curve fitting to the axial and radial flux profiles. A reflector savings for the ZPR-3 depleted-uranium axial blanket was derived from the measured axial buckling and core height. Savings for steel and aluminum were then obtained by using the worths found in axial-reflector experiments. The $^{235}U/^{238}U$ fission ratio in the equilibrium spectrum of the exponential is compared in Table XXIX with the ratio measured at the center of Assembly 41.

The difference between the bucklings found in the two systems is difficult to understand. Fundamental-mode calculations with several cross-section sets give bucklings more on the order of the Assembly 41 determination than that given by the exponential experiment. For the reflector savings, a quantitative comparison of values between the systems is not valid, considering the differences in reflector compositions and directional bucklings. However, a qualitative comparison does show a disagreement about the effectiveness of aluminum, relative to uranium and steel, as a reflector. These anomalies tend to confirm some conclusions of Reardon and Hummel[10] that direct leakage of source neutrons through the reflectors on the exponential piles distorted the fluxes and gave improper directional bucklings.

# XII. ASSEMBLY 41 RESULTS COMPARED WITH RELEVANT MEASUREMENTS IN A FAST-THERMAL CRITICAL EXPERIMENT (ZPR-5)

## A. Details of Fast-Thermal Reactor

The 5/1 uranium composition for the exponential experiment cited in Section XI was also the subject of an investigation as an "internal exponential," that is, as the central zone of a coupled fast-thermal system.[11] This study was conducted in ZPR-5 at Argonne, Illinois, as a follow-on to the exponential experiment; the purpose was to measure material reactivity coefficients, foil activations, and spectrum for the 5/1 composition. Figure 41 is a diagram of the coupled reactor showing the fast central zone surrounded by a natural-uranium blanket and a thermal $^{235}U$ driver zone. The investigations with this reactor system included studies of coupling between the fuel zones and the effectiveness of various spectrum-filtering zones between the fuel zones. The measurements comparable to related Assembly 41 experiments included reactivity coefficients and fission ratios at the core center.

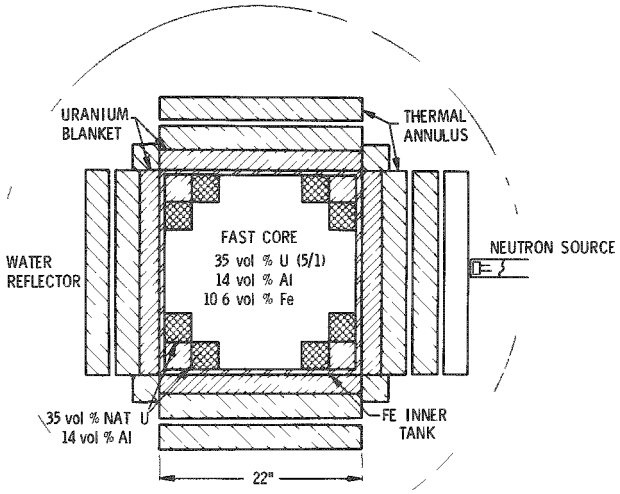


Fig 41. ZPR-5 Fast-Thermal Experiment. ANL Neg. No. 103-2285.

## B. Comparison of Measurements in ZPR-3 Assembly 41 with Those in ZPR-5

The $^{235}U/^{238}U$ central fission ratio found in ZPR-5 was 24.8 ± 1.1, in good agreement with the exponential experiment and Assembly-41 values. Material reactivity worths at the core centers in Assembly 41 and ZPR-5 are compared in Table XXX; the experimental values in each case have been normalized to a perturbation cross section for $^{235}U$ which was calculated with ANL cross-section set 635 and central fluxes from a transport-theory calculation. The table also gives calculated perturbation cross sections for a number of other materials.

Except for the fissile materials and $^{10}B$, the experimental errors associated with the Assembly 41 results in Table XXX are about ±5 millibarns. In general, the coefficients from the 5/1, fast-thermal system differ from the Assembly 41 data by 5 or more millibarns. The differences in material worths (actually in worths relative to $^{235}U$ worth) between the two systems

is probably not due to the minor differences in core composition. Rather, the disagreements reflect differences in the techniques used for the measurements; the most probable factor is differences in sample size with correspondingly different shielding and multiple-scattering effects. However, the results may also indicate that the fast zone in the coupled system was not sufficiently large or buffered enough from the thermal region, giving central real and adjoint spectra unrepresentative of the spectra in an extensive fast zone.

TABLE XXX. Comparison of Material Worths Measured in the 5/1 Uranium Fast Cores and Calculated by Perturbation Theory

| | Reactivity Coefficient, millibarns | | |
|---|---|---|---|
| Material | Measured in ZPR-3 Assembly 41 | Measured in ZPR-5 Fast-Thermal Assembly | Calculated by Perturbation Theory |
| $^{235}U$ | 1865 | 1865 | 1865 |
| $^{238}U$ | -86 | - | -80 |
| Silver | -276 | -300 | - |
| Aluminum | -8 | -4 | -7 |
| $^{10}B$ | -1100 | -971 | -794 |
| Bismuth | -18 | -18 | - |
| Carbon | +1 | $<4$ | 0 |
| Iron | -16 | -27 | -20 |
| Sodium | +1 | - | -1 |
| Nickel | -24 | -45 | - |
| Sulfur | -40 | -48 | - |
| Tin | -52 | -63 | - |
| Tantalum | -276 | - | -240 |
| Tungsten | -119 | -141 | - |
| Zirconium | -23 | -39 | -29 |

# APPENDIX A

## Assembly 41 Drawer Loadings

Figures 5 and 6 show the loading patterns for the various types of core and blanket drawers used in the Assembly 41 critical configuration; Fig. 3 shows the loadings of material columns in the four types of core drawers in the basic core cell.

The masses of materials loaded into these core and blanket drawers are specified in Table XXXI. The regular core drawers were 21 in. long, and the specifications given for the 16-in. core section at the front include the drawer front and the matrix and drawer steel. Axial blanket was included in the back of the front drawer and in the front 7 in. of an 11-in. backup drawer. For the control-rod drawers, with the types and positions as indicated in Figs. 5 and 6, the core-section loadings given in Table XXXI include the heavier rod structure and a partition at 15 in.; there were three type 2 control rods (with two columns of fuel) and a total of seven of types 1, 3, and 4 (with one column of fuel). The inner radial blanket region shown in Figs. 5 and 6 contained uranium bricks in 21-in. front drawers backed up by 7 in. of bricks in the matrix. In the outer radial blanket, all 28 in. of uranium blanket was loaded directly into the matrix.

TABLE XXXI. Specifications of Drawer Loadings Used in Assembly 41 Reference Configuration

| Drawer Type, Section | Section Length,[a] cm | Section Loading of Materials, kg | | | |
|---|---|---|---|---|---|
| | | Enriched Uranium[b] | Depleted Uranium[c] | Stainless Steel[d] | Aluminum |
| Type 1 core | 40.72 | 1.1670 | 7.1480 | 1.3789 | 0.6030 |
| Type 2 core | 40.72 | 2.3239 | 5.9418 | 1.3792 | 0.6022 |
| Type 3 core | 40.72 | 1.1670 | 7.1480 | 1.3789 | 0.6030 |
| Type 4 core | 40.72 | 1.1654 | 7.1480 | 1.3789 | 0.6030 |
| Type 1, 3, and 4 core control drawer | 40.95[e] | 1.1670 | 7.1423 | 1.554 | 0.6063 |
| Type 2 core control drawer | 40.95[e] | 2.3341 | 5.9519 | 1.554 | 0.6063 |
| Axial blanket in front drawers | 12.70 | - | 6.1621 | 0.2750 | - |
| Spring gap[f] | 0.66 | - | - | 0.043 | - |
| Axial blanket in back drawers | 17.78 | - | 8.6225 | 0.3850 | - |
| Control drawer axial blanket | 30.48 | - | 14.785 | 1.1167 | - |
| Inner radial blanket | 53.42 | - | 25.866 | 1.166 | - |
| Outer radial blanket | 71.12 | - | 34.490 | 15.575 | - |

[a]Matrix unit 5.5461 cm wide by 5.5258 cm high.
[b]93.26 wt % $^{235}U$, 5.39 wt % $^{238}U$, 0.95 wt % $^{234}U$, 0.40 wt % $^{236}U$.
[c]0.206 wt % $^{235}U$.
[d]73.4 wt % Fe, 17.0 wt % Cr, 8.4 wt % Ni, 0.75 wt % Mn, 0.45 wt % Si.
[e]0.16-cm partition in control drawer intersects core section at 38.1 cm.
[f]Composed of spring in end of 21-in. drawer, drawer back, and front of back drawer.

# APPENDIX B

## Specifications of Core Heterogeneity for Assembly 41

The loadings of the core drawers in each half of ZPR-3 are composed of material plates of various thicknesses aligned into columns with axial lengths of half the core length. The pattern of different columns across the reactor is a repetition of the basic-cell loading that defines the core composition. Thus, the overall heterogeneity of the core is defined by the plate arrangement in the basic cell. For Assembly 41, the basic cell was the four-drawer loading shown in Fig. 3, containing five columns of enriched uranium dispersed evenly among various diluent plates.

The stack of columns in each of the four sections of the cell had a cross section of 2 x 2 in., the nominal inside dimensions of the stainless steel drawers containing the stack. The drawers are further separated by the walls of the reactor matrix tubes. Figure 42 gives the actual geometries and densities of these structural components. For simplicity, however, the 2 x 2-in. stacks of columns in the drawers can be considered bounded by vertical and horizontal walls of structure, as shown in Fig. 43, with the average compositions given in Table XXXII.

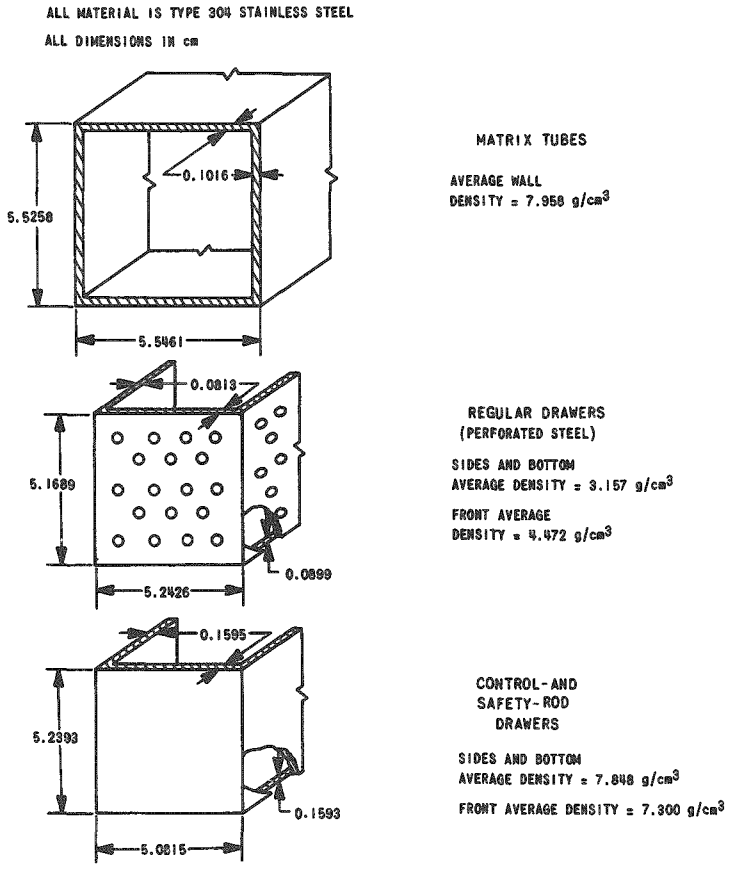


Fig. 42. ZPR-3 Matrix and Drawer Geometries. ANL Neg. No. 103-2959.

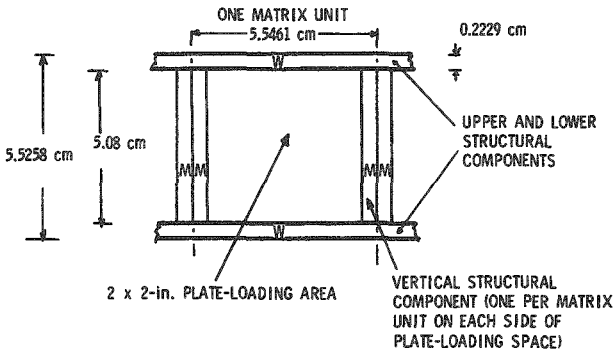


Fig. 43

Homogenized Representation of ZPR-3 Structural Components

TABLE XXXII. Specifications of Cell-constituent Columns for Assembly 41 Core

| | Structure Component or Material Column | | | | | | | |
|---|---|---|---|---|---|---|---|---|
| Type: | Horizontal Structure Wall[a] | Vertical Structure Wall[b] | 1/16-in. Enriched Uranium | 1/8-in. Enriched Uranium | 1/8-in. Depleted Uranium | 1/16-in. Depleted Uranium | 45 vol % Aluminum | Stainless Steel |
| Thickness, cm: | 0.2229 | 0.2331 | 0.1588 | 0.3175 | 0.3175 | 0.1588 | 0.3175 | 0.3175 |
| Column-average Density, $10^{22}$ atoms/cm$^3$ | | | | | | | | |
| $^{235}U$ | - | - | 4.2434 | 4.2384 | 0.0096 | 0.0096 | - | - |
| $^{238}U + ^{236}U$ | - | - | 0.2603 | 0.2600 | 4.5600 | 4.5600 | - | - |
| $^{234}U$ | - | - | 0.0434 | 0.0434 | - | - | - | - |
| Aluminum | - | - | - | - | - | - | 2.5613 | - |
| Iron | 3.5159 | 3.6464 | - | - | - | - | - | 5.9224 |
| Chromium | 0.8746 | 0.9071 | - | - | - | - | - | 1.4733 |
| Nickel | 0.3828 | 0.3970 | - | - | - | - | - | 0.6447 |
| Manganese | 0.0365 | 0.0379 | - | - | - | - | - | 0.0615 |
| Silicon | 0.0429 | 0.0444 | - | - | - | - | - | 0.0722 |

[a]Includes bottom and top of matrix and bottom of drawer, represented by W in Fig. 43.
[b]Includes sides of matrix and drawer, represented by M in Fig. 43.

Table XXXII includes the specifications of the various 1/8-in.-thick columns of fuel and diluents used in the loadings of the basic core drawers, and also of the 1/16-in.-thick uranium columns involved in unbunching experiments (see Section III). The specifications are idealized to the extent of assuming nominal plate heights and widths and including the void content from slack into the structure components.

# APPENDIX C

## Delayed-neutron Parameters and Absolute Reactivity Calibration

Reactivity measurements in Assembly 41 were obtained with control rods which were calibrated in inhours by a series of period measurements. The period values were converted into reactivity increments for the associated rod segments by means of a period-to-inhour curve appropriate to the assembly composition. With the use of real and adjoint fluxes from a diffusion-theory calculation for Assembly 41, a code for averaging the delayed-neutron productions provided an effective delayed-neutron fraction of 0.00733 and an equivalence of 440 Ih per % $\Delta k/k$. These values indicate that the delayed neutrons have effective portions as follows. 29% from fissions in $^{238}U$ and 71% from fissions in $^{235}U$.

For an asymptotic period T, in the range of the measurements, the reactivity is given by

$$\frac{\Delta k}{k} = \beta_{eff}\left( {}^{25}C\sum_{i=1}^{6}\frac{a_i^{25}}{1+T\lambda_i^{25}} + {}^{28}C\sum_{i=1}^{6}\frac{a_i^{28}}{1+T\lambda_i^{28}}\right),$$

where $^{25}C$ and $^{28}C$ are the effective portions of the delayed neutrons from $^{235}U$ and $^{238}U$, respectively, $a_i$ is the fraction of delayed neutrons in group i, and $\lambda_i$ is the decay constant for group i. The conversion to inhours is obtained by multiplying by $4.4 \times 10^5$ (the reciprocal of $\Delta k/k$ for T = 3600 sec). For the periods involved, the reactivities in inhours do not depend on $\beta_{eff}$ and are relatively insensitive to variance in $^{28}C$ versus $^{25}C$. Therefore the experimental worths obtained in inhours should be as accurate as the calibrations. Conversion of the experimental worths to $\Delta k$ for correlation with calculations, however, has the uncertainty associated with the error in calculated $\beta_{eff}$. Table XXXIII lists the delayed-neutron parameters used in the calculations.

TABLE XXXIII. Delayed-neutron Specifications for Assembly 41

$\beta_{eff}$ = 0.00733 $^{25}C$ = 0 71, $^{28}C$ = 0.29

| | Delayed-neutron Parameters | | | |
|---|---|---|---|---|
| | $^{235}U$ | | $^{238}U$ | |
| Delayed Group i | $a_1$ | $\lambda_i$, $sec^{-1}$ | $a_i$ | $\lambda_1$, $sec^{-1}$ |
| 1 | 0 038 | 0 0127 | 0 013 | 0.0132 |
| 2 | 0.213 | 0.0317 | 0 137 | 0 0321 |
| 3 | 0.188 | 0.115 | 0.162 | 0.139 |
| 4 | 0.407 | 0.311 | 0.388 | 0.358 |
| 5 | 0.128 | 1.400 | 0.225 | 1 410 |
| 6 | 0.026 | 3.870 | 0.075 | 4.020 |

Table XXXIV lists the period measurements carried out for the reactivity of various segments of a control rod. Overall, the calibrations in inhours have an accuracy of about ±1%, which would pertain also to all worth measurements. Figure 44 is a plot of the rod calibration obtained.

TABLE XXXIV. Period Measurements for Rod Calibrations

| Measurement No. | Rod Increment, in. | Period, T, sec | Worth, Ih |
|---|---|---|---|
| 1 | 2.614 to 0.00 | 125.85 ± 2 | 23.14 ± 0.4 |
| 2 | 2.933 to 0.00 | 107.2 ± 1.5 | 26.31 ± 0.4 |
| 3 | 3.415 to 0.00 | 87.3 ± 1.0 | 31.02 ± 0.4 |
| 4 | 5.951 to 2.933 | 96.0 ± 1.0 | 28.70 ± 0.4 |
| 5 | 7.912 to 5.951 | 173.8 ± 3.0 | 17.66 ± 0.4 |

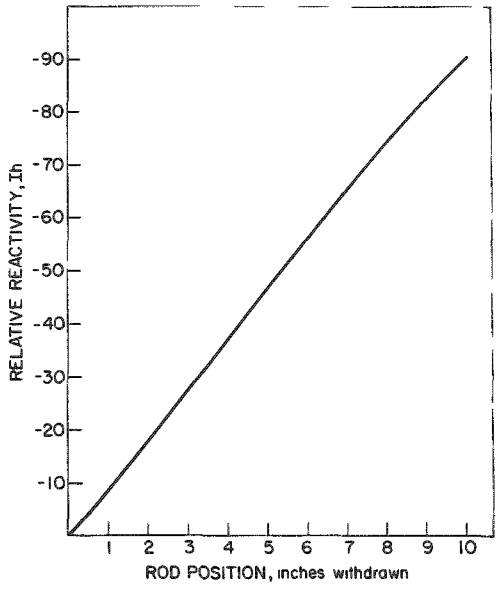


Fig. 44

Calibration of ZPR-3 Control Rod No. 10

# APPENDIX D

## Description of Neutron Detectors for Reaction-rate Traverses

Fission-rate profiles in the ZPR-3 assemblies have been obtained primarily by traversing small, cylindrical fission counters designed by W. C. Redman of the ANL Applied Physics Division. For the $^{10}B$ reaction, traverses have been run with small-diameter $BF_3$ counters. In these measurements, the reactor perturbation has been minimized by using a 1/2-in.-dia traverse channel.

A Redman counter basically consists of a $1\frac{1}{4}$-in.-long plating of fissile material on the inside of a 7/16-in.-dia brass annulus, a central collector anode, and a sealed-in mixture of argon and methane. For the $BF_3$ counter, the gas chamber is about 2 in. long and 3/8 in. in diameter. Loading specifications for the traverse counters used in Assembly 41 are given in Table XXXV. Diagrams for the basic counter designs are given in Fig. II.B.8 of the Reactor Development Program Progress Report for May 1968, ANL-7457, p. 23.

TABLE XXXV. Specifications of Fission and $BF_3$ Traverse Counters

| Counter Type | Composition of Reactive Material | Loading of Reactive Material |
|---|---|---|
| Redman J, Enriched U Fission | 93.2 wt % $^{235}U$, 6 wt % $^{238}U$, 0.8 wt % $^{234}U$ | 5.1 mg (0.60 mg/cm$^2$)[a] |
| Redman K, $^{234}U$ Mixture Fission | 89.34 wt % $^{234}U$, 7.72 wt % $^{235}U$, 2.89 wt % $^{238}U$ | 2.8 mg (0.33 mg/cm$^2$)[a] |
| Redman IC-24-1, $^{238}U$ Fission | 80 ppm $^{235}U$ | ~4.8 mg (0.56 mg/cm$^2$)[a] |
| Nancy Wood G-15758 $^{10}B(n,\alpha)$ | About 90 at. % $^{10}B$ in boron of $BF_3$ | $BF_3$ filling[b] to pressure of about 20 cm Hg. |

[a] Annular plating, 0.84-cm diameter x 3.21 cm long.
[b] Cylindrical chamber inside dimensions, about 0.95-cm diameter x 5.0 cm long.

## ACKNOWLEDGMENTS

As with other assemblies in ZPR-3, the successful implementation of the experimental program involved the combined efforts of administrators, experimentalists, technicians, and clerical personnel, and their contributions are genuinely appreciated. The authors provided the specific design of the experiments and supervised the operations. Thanks are due to F. W. Thalgott and W. Loewenstein for overall program guidance and helpful suggestions. Recognition is also given to G. S. Brunson for the Rossi-alpha measurements and to E. Slansky for assistance in data reduction.

## REFERENCES


1. B. C. Cerutti *et al.*, *ZPR-3, Argonne's Fast Critical Facility*, Nucl. Sci. Eng. *1*, 126 (1956).
2. J. K. Long *et al.*, "Fast Neutron Power Reactor Studies with ZPR-3," Proc. U.S. International Conference on Peaceful Uses of Atomic Energy *12*, 119 (1958).
3. W. G. Davey, *An Analysis of 23 ZPR-III Fast-reactor Critical Experiments*, Nucl. Sci. Eng. *19*, 259 (1964).
4. G. S. Brunson *et al.*, *Measuring the Prompt Period of a Reactor*, Nucleonics *15*, (No. 11), 32 (1957).
5. F. S. Kirn, *An Absolute Fission Counter*, American Nuclear Society, 2nd Winter Meeting (1957).
6. W. G. Davey and P. I. Amundson, *A Re-evaluation of Fission Ratios Measured in ZPR-III Critical Assemblies*, ANL-6941 (Oct 1964)
7. L. J. Koch *et al.*, *Hazards Summary Report: Experimental Breeder Reactor II (EBR-II)*, ANL-5719 (May 1957).
8. W. G. Davey, *k Calculations for 22 ZPR-III Fast Reactor Assemblies Using ANL Cross-section Set 635*, ANL-6570 (May 1962).
9. F. H Martens, *The Fast Exponential Experiment*, ANL-5379 (Nov 1955).
10. W. A. Reardon and H. H. Hummel, *A Study of the Equilibrium Process in the Fast Exponential Experiment*, Nucl. Sci. Eng. *3*, 201-213 (1958).
11. H. H. Hummel *et al.*, "Experimental and Theoretical Studies of the Coupled Fast-thermal System ZPR-V," *Proc. International Conference on Peaceful Uses of Atomic Energy 12*, Geneva, 1958, Paper No. 599, p. 166